Stability and Chaotic Analysis of Nonlinear Fractional Model Using Novel Analytical Technique: Soliton Solutions for Wazwaz Kaur Boussinesq Equation

Amna Mumtaz[1],Muhammad Shakeel[1], Abdul Manan[2] and Nehad Ali Shah[3,*]

[1] Department of Mathematics, University of Wah, Wah Cantonment, 47040, Pakistan

[2] Department of Mathematics, Faculty of Sciences, Superior University, Lahore, 54000, Pakistan

[3] Department of Mechanical Engineering, Sejong University, Seoul, 05006, Republic of Korea

Revista Internacional
Métodos numéricos
para cálculo y diseño en ingeniería

RIMNI

UNIVERSITAT POLITÈCNICA DE CATALUNYA BARCELONATECH

In cooperation with CIMNE

INFORMATION

Keywords:
Novel modified (G'/G^2)-expansion approach
Wazwaz Kaur Boussinesq equation
conformable derivative
M-truncated derivative
β-derivative
phase portrait
Poincaré map

DOI: 10.23967/j.rimni.2025.10.64345

Revista Internacional de Métodos Numéricos para Cálculo y Diseño en Ingeniería

Stability and Chaotic Analysis of Nonlinear Fractional Model Using Novel Analytical Technique: Soliton Solutions for Wazwaz Kaur Boussinesq Equation

Amna Mumtaz[1], **Muhammad Shakeel**[1], **Abdul Manan**[2] **and Nehad Ali Shah**[3,*]

[1]Department of Mathematics, University of Wah, Wah Cantonment, 47040, Pakistan

[2]Department of Mathematics, Faculty of Sciences, Superior University, Lahore, 54000, Pakistan

[3]Department of Mechanical Engineering, Sejong University, Seoul, 05006, Republic of Korea

ABSTRACT

This study examines the exact solutions of the nonlinear Wazwaz-Kaur Boussinesq (NLWKB) equation in $(2+1)$-dimension by using a novel modified (G'/G^2)-expansion method. This examination uses Beta-Derivative, M-Truncated and Conformable derivatives for finding new closed-form soliton solutions. The graphic demonstration covers some of these solutions. These visualized graphs show individual W-type, bright, and dark solitons to emphasize the effect of fractional derivatives on the behavior of waves. Furthermore, the study investigates the bifurcation analysis, chaotic dynamics, multistability, and Poincaré maps to describe the stability transitions of the system. The results illustrate how fractional calculus improves soliton modeling and nonlinear wave propagation, with possible applications in plasma physics, optical fiber communications, ion-acoustic, magneto-sound, and stationary media, and wave dynamics in complex media, and the transmission of tidal and tsunami waves. The proposed method proves to be a powerful method for solving nonlinear fractional models and examining their dynamic behavior.

OPEN ACCESS

Received: 12/02/2025

Accepted: 15/04/2025

Published: 30/05/2025

DOI
10.23967/j.rimni.2025.10.64345

Keywords:
Novel modified (G'/G^2)-expansion approach
Wazwaz Kaur Boussinesq equation
conformable derivative
M-truncated derivative
β-derivative
phase portrait
Poincaré map

1 Introduction

Nonlinear partial differential equations of fractional order have an important part in engineering and science as they efficiently describe numerous nonlinear phenomena. Finding exact solutions of these equations is crucial for understanding their nonlinear properties, which pushes mathematicians to discover appropriate analytical techniques for solving both linear and nonlinear differential equations. Over the previous few years, fractional partial differential equations and fractional calculus have attained notable consideration because of their wide uses in many fields, including plasma physics,

*Correspondence: Nehad Ali Shah (nehadali199@sejong.ac.kr).

mathematical physics, finance, biology, engineering, mechanics, and electrochemical processes [1]. Fractional calculus extends classical calculus by introducing integration and differentiation of non-integer orders, giving a strong structure for modeling systems with long-term interactions, memory effects, and nonlocal behaviors. In this framework, the fractional derivative—usually considered an extension of the integral—is generalized to contain non-integer and even complex orders, leading to the improvement of novel mathematical methods to deal with fractional-order differential equations. Several real-world phenomena that diverge from classical integer-order models can be better demonstrated by using such equations.

The conduct of fractional partial differential equations and their solutions has been widely analyzed in many models, including the special time-fractional model [2], the fractional Klein-Gordon equation [3], the Boussinesq equation [4], the Allen-Cahn and fractional-order Phi-4 equation [5], the fractional advection-dispersion equation [6], the time-fractional simplified Camassa-Holm equation [7], the fractional Camassa-Holm equation [8], and, the fractional Burger's equation [9], among others. Fractional derivatives have also been used in a wide range of materials and polymer processes, capturing genetic characteristics and memory effects. Given the complex structures of polymers—materials that frequently display nonlocal effects, memory-dependent responses, and time-dependent behaviors—fractional calculus offers a complete method to model their complex properties. Recent studies have discovered several fractional derivative operators, including the Atangana beta and conformable derivatives [10], the Caputo fractional derivative [11], the ψ-Hilfer fractional derivative [12], the k-Riemann-Liouville derivative [13], and the Modified Riemann-Liouville derivative [14].

Because of the intrinsic complexity of fractional partial differential equations (PDEs), finding their exact solutions is often difficult. Therefore, researchers have established many analytical approaches to overcome this difficulty. Some of the commonly used methods include the Modified F-expansion approach [15], the Tanh-function technique [16], the inverse scattering transform method [17], the exp-function method [18], the modified exp-function method [19–21], the extended exp-function method [22], the $\exp(-\Phi(\eta))$-expansion method [23], and the multiple exp-function method [24]. The (G'/G^2)-expansion method has also been widely used in the latest studies. For example, Arshed and Sadia [25] employed this technique to obtain soliton solutions for three different fractional-order nonlinear models. Similarly, Nisar et al. used an extended version of the (G'/G^2)-expansion methodology to the Heisenberg ferromagnetic spin chain model in $(2+1)$-dimension, leading to the discovery of new soliton solutions [26]. Based on this progress, the current research uses a recently developed novel modified (G'/G^2)-expansion method to derive exact solutions for fractional partial differential equations. This novel method, developed by Mumtaz et al. [27], has illustrated important developments in solving nonlinear fractional systems, mainly in finding soliton solutions.

The (G'/G^2)-expansion method has attained momentous attention due to its capability to derive exact solutions for differential equations, including both temporal and spatial fractional orders. This technique emphasizes generating closed-form solutions for a number of fractional-order differential equations and gives a strong analytical framework. In this toil, we discover new fractional solutions by using the new expansion method, called the novel modified (G'/G^2)-expansion, together with the three different derivatives to investigate the nonlinear WKB equation in $(2+1)$-dimension. The fractional order β-Derivative includes beta function parameters, giving an alternative differentiation method that improves computational flexibility. Compared to regular fractional derivatives, the β-derivative makes fractional differentiation simpler, making it more flexible and effective for solving nonlinear fractional models. However, it remains comparatively less analyzed in contrast to other fractional derivatives, guaranteeing further investigation of its potential applications.

Recent research in optical solitons and nonlinear wave equations has highlighted the increasing importance of fractional derivatives in modeling complex systems [28,29]. The utilization of fractional derivatives has improved the accuracy of soliton modeling in both plasma physics and optical fiber communication. Moreover, the *l*atest investigations [30,31] demonstrate the increasing importance of fractional solitons in optical and plasma physics. Younas et al. [32] investigated the chaotic structure and sensitivity exploration of solitons in nonlinear fractional longitudinal wave equations and focused on the effects of different initial conditions and parameters. In the same way, Ismael et al. discovered the dynamic wave behavior in a generalized (3 + 1)-dimensional Kadomtsev-Petviashvili equation, improving the comprehension of nonlinear wave behavior in higher-dimensional models [33].

Bifurcation analysis, chaos analysis, multistability, and Poincare mapping are important techniques for analyzing dynamic behavior in systems such as the Heimburg model. Bifurcation analysis can provide insight into how small changes in parameters lead to significant changes in state, indicating transitions between stable and unstable behavior. Time series analysis complements this by following the time evolution of solitons, helping to identify patterns, stability, and oscillatory behavior. Chaotic analysis explores the strong sensitivity to initial conditions and the emergence of strange attractors, where small changes in initial conditions give rise to unpredictable and aperiodic trajectories. It aids in identifying whether a system shows deterministic chaos, oscillates between periodic-to-chaotic transitions, or maintains a quasi-periodic trajectory [34–37]. On the other hand, multistability denotes the coexistence of multiple stable states within the same parameter set, where distinct initial conditions give rise to different attractors. Chaos emphasizes unbounded complexity and irregular trajectories, whereas multistability focuses on the system's tendency to stabilize in different attractors based on initial conditions rather than unpredictability [38,39]. Poincaré map further elucidates this behavior using Poincaré sections [40]. Collectively, these techniques provide a framework for understanding complex soliton dynamics in nonlinear models.

In this study, to obtain the solutions of the nonlinear Wazwaz Kaur Boussinesq equation in (2 + 1)-dimension, the novel modified (G'/G^2)-expansion method in conjunction with beta, M-truncated, and conformable derivatives has been employed [41–44]. Additionally, the dynamics analysis of the Wazwaz-Kaur Boussinesq equation explores transitions between stable and chaotic states using bifurcation diagrams, chaos analysis, multistability analysis, and Poincaré maps. Bifurcation analysis identifies parameter-driven shifts in stability, while chaos analysis quantifies unpredictable behavior. Multistability reveals the coexistence of multiple attractors, demonstrating the system's sensitivity to initial conditions. The Poincaré map simplifies the visualization of complex trajectories, distinguishing periodic from chaotic solutions. Together, these methods provide a comprehensive understanding of the equation's dynamic behavior across different regimes. Applications for this nonlinear equation include optical fiber, contemporary communication network technologies, homogeneous stationary media, plasma physics, and tidal and tsunami wave propagation.

Soliton solutions to nonlinear equations are broadly studied with various analytical techniques. Many researchers have examined the Wazwaz Kaur Boussinesq equation in (2 + 1)-dimension by different analytical and numerical methods. However, the former methods mainly focused on integer-order derivatives, restricting the capability to model memory effects and nonlocal interactions, which are important fields in wave propagation in the real world. The novelty of this study is the application of the novel modified (G'/G^2)-expansion method together with fractional derivatives (β, M-Truncated and Conformable) covers classical soliton models and offers an expanded range of solutions, including bright, dark, and W-type solitons. In contrast to classical methods, our method provides more adaptable and generalized solutions, enhancing its effectiveness in modeling nonlinear wave dynamics

The soliton solutions obtained in this study have potential uses in fluid dynamics, optical solitons, and materials science. In fluid mechanics, the results can model nonlinear shallow water wave propagation and tidal wave interactions. In optical fiber communications, soliton solutions describe pulse transmission through nonlinear dispersive media. Moreover, in materials science, fractional soliton models aid in understanding nonlinear wave behavior in complex materials, such as polymer structures and nanomaterials. These applications illustrate the importance of studying outside theoretical mathematics.

In spite of major developments in solving fractional nonlinear PDEs, existing methods often fail to capture the complex soliton structures arising in perturbed nonlinear systems. This study fills this gap by introducing a novel modified (G'/G^2)-expansion method, which is applied to the $(2+1)$-dimensional WKB equation for the first time. This method not only derives new soliton solutions but also analyzes their stability, bifurcation analysis, and chaotic behavior, providing a deeper knowledge of nonlinear fractional systems.

This study aims to obtain precise soliton solutions of the nonlinear Wazwaz-Kaur Boussinesq (WKB) equation in $(2+1)$ dimension using a novel modified (G'/G^2)-expansion method. Moreover, this study examines the system's bifurcation, chaotic behavior, and multistability to investigate its sensitivity to initial conditions. The fractional derivatives used in this work are: Conformable Derivative: A fractional derivative that preserves the chain rule and offers a simple extension of classical differentiation. M-Truncated Derivative: Used to approximate nonlinear fractional models, providing a computational advantage in solving fractional partial differential equations. β-Derivative: A comparatively new fractional operator that includes the Beta function, allowing for improved adaptability in catching memory and transmissible features of nonlinear systems. The application of these three derivatives together with the novel modified (G'/G^2)-expansion method discovers many soliton solutions, providing understandings into their physical properties and stability under perturbations. The comparison of the solutions obtained is also provided in the form of Table 1.

The proposed novel modified (G'/G^2)-expansion method extends the classical (G'/G)-expansion method and offers several advantages, including the flexibility of solutions to nonlinear integer order and fractional order differential equations and the ability to generate a wide range of soliton solutions. This method provides a highly important and exact analytical solution for understanding complex nonlinear dynamics and validation of numerical simulations. Its applicability extends to fields such as plasma physics, optical fiber communications, and fluid dynamics, where nonlinear wave phenomena are preferred. Additionally, it facilitates a wide range of dynamic analysis, including bifurcation, chaos, and multistability, providing deep insight into system behavior and stability.

This study is organized into eleven sections for a comprehensive exploration of the subject. Section 2 introduces the concept of different fractional derivatives. Section 3 states the process of the suggested method. Section 4 presents the use of the method along with the resulting outcomes, while section 5 focuses on the graphical representation and confab of the outcomes. Section 6 delves into bifurcation analysis, followed by Section 7, which examines chaotic behavior. Section 8 explores time-series analysis, and Section 9 investigates the phenomenon of multi-stability. Section 10 discusses the Poincaré map, and finally, Table 1 concludes the study with a summary of key insights and implications.

Table 1: Comparison of our solutions and the solutions by Saboor et al. [44]

Our solutions	Solutions by Saboor et al. [44]
If we put $H=0, A=1, B=1, C=0, P=0, l=1,$ $m=1, k=1, n=2$ and $w_{101}(\eta)=\vartheta_{1a}(\psi)$ in (71), then $\vartheta_{1a}(\psi)=\frac{2\left(2\cos^2(\psi)+1\right)}{\cos^2(\psi)-1}$.	If we put $\upsilon=1, \Lambda=1, Y=0, \varphi_1=0, x_1=1, x_2=1,$ $x_3=2, u=1$ in (4.33), then $\vartheta_{1a}(\psi)=\frac{2\left(2\cos^2(\psi)+1\right)}{\cos^2(\psi)-1}$.
If we put $H=0, A=-1/2, B=1/2, C=0, P=1,$ $Q=1, l=1, m=1, k=1, n=2$ and $w_{102}(\eta)=\vartheta_{1b}(\psi)$ in (72), then $\vartheta_{1b}(\psi)=\frac{2-\cos h(\psi)}{1+\cos h(\psi)}$.	If we put $\upsilon=-1/2, \Lambda=1/2, \Upsilon=0, \varphi_1=1, \varphi_2=1, x_1=1,$ $x_2=1, x_3=2, u=1$ in (4.34), then $\vartheta_{1b}(\psi)=\frac{2-\cos h(\psi)}{1+\cos h(\psi)}$.
If we put $H=0, A=1, B=1, C=1, P=1,$ $Q=1, l=1, m=1, k=1, n=1$ and $w_{103}(\eta)=\vartheta_{1c}(\psi)$ in (73), then $\vartheta_{1c}(\psi)=-3\left(2\psi^2+2\psi+1\right)$.	If we put$\upsilon=1, \Lambda=1, \Upsilon=1, \varphi_1=1, \varphi_2=1, x_1=1, x_2=1, x_3=1, u=1$ in (4.35), then $\vartheta_{1c}(\psi)=-3\left(2\psi^2+2\psi+1\right)$.
If we put $H=0, A=3, B=1, C=4, Q=0, l=1,$ $m=-1, k=1, n=2$ and $w_{104}(\eta)=\vartheta_{1d}(\psi)$ in (74), then $\vartheta_{1d}(\psi)=\frac{4(5\cos h(2\psi)+4\sin h(2\psi)+6)}{5\cos h(2\psi)+4\sin h(2\psi)-3}$.	If we put $\upsilon=3, \Lambda=1, \Upsilon=4, \varphi_2=0, x_1=1, x_2=-1,$ $x_3=2, u=1$ in (4.36), then $\vartheta_{1d}(\psi)=\frac{4(5\cos h(2\psi)+4\sin h(2\psi)+6)}{5\cos h(2\psi)+4\sin h(2\psi)-3}$.
If we put $H=0, A=1, B=2, C=2, Q=0, l=1,$ $m=1, k=1, n=2$ and $w_{105}(\eta)=\vartheta_{1e}(\psi)$ in (75), then $\vartheta_{1e}(\psi)=\frac{4(\sin(2\psi)-2)}{\sin(2\psi)+1}$.	If we put $\upsilon=1, \Lambda=2, \Upsilon=2, \varphi_2=0, x_1=1, x_2=1,$ $x_3=2, u=1$ in (4.37), then $\vartheta_{1e}(\psi)=\frac{4(\sin(2\psi)-2)}{\sin(2\psi)+1}$.

2 Preliminaries

This section provides an overview of the derived definitions and their most important features.

Beta Derivative: Let $w\colon [y,\infty)\to\Re$, $t\geq 0$, $y\in\Re$ be a continuous function. The β fractional derivative is defined as [41]:

$$D^{\beta}w(t)=\lim_{\zeta\to 0}\frac{w\left(t+\zeta\left(t+\frac{1}{\Gamma(\beta)}\right)^{1-\beta}\right)-w(t)}{\zeta},\ \text{where } \beta\in(0,1]$$

where the gamma function Γ is defined as: $\Gamma(\upsilon)=\int_0^{\infty}t^{\upsilon-1}e^{-t}dt$.

Let the differential functions $\gamma(t)$ and $\delta(t)$ having order $0<\beta\leq 1$ and $t\geq 0$, then:

i) $D^{\beta}(a\gamma(t)+b\delta(t))=aD^{\beta}(\gamma(t))+bD^{\beta}(\delta(t)), \forall a, b\in\Re$.

ii) $D^{\beta}(a\gamma(t)b\delta(t))=\gamma(t)D^{\beta}(\delta(t))+\delta(t)D^{\beta}(\gamma(t))$.

iii) $D^{\beta}\left(\frac{\gamma(t)}{\delta(t)}\right)=\frac{\gamma(t)D^{\beta}(\delta(t))-\delta(t)D^{\beta}(\gamma(t))}{\delta(t)^2}$.

iv) $D^{\beta}(p) = 0$, for any constant p.

v) Considering $\lambda = \left(t + \frac{1}{\Gamma(\beta)}\right)^{1-\beta} \theta$, where $\theta \to 0$ when $\lambda \to 0$, therefore we get:

$$D^{\beta}(\delta(t)) = \left(t + \frac{1}{\Gamma(\beta)}\right)^{1-\beta} \frac{d\delta(t)}{dt},$$

with $\chi = \frac{c}{\beta}\left(t + \frac{1}{\Gamma(\beta)}\right)^{\beta}$. The properties of β fractional derivative are confirmed in the research [42].

M-Truncated Derivative:

Let $w: [y, \infty) \to \Re$ having order $\beta \in (0, 1]$, then M-Truncated fractional derivative is defined as [43]:

$$D^{\beta}_{M,t} w(t) = \lim_{\alpha \to 0} \frac{w(t + \gamma E_{\delta}(\alpha t^{-\beta})) - w(t)}{\alpha}, \; t > 0,$$

and $\gamma E_{\delta}(.)$ is the Mittag-Leffler truncated function in solo parameter is demarcated below [44,45]:

$$\gamma E_{\delta}(t) = \sum_{i=0}^{k} \frac{t^{i}}{\Gamma(\delta i + 1)}.$$

Theorem 1: Let $\beta \in (0, 1]$, $\delta > 0, \gamma_1, \gamma_2 \in \Re$ and K, L be differential functions of order β.

i) $D^{\beta}_{M,\chi}(\gamma_1 K(\psi) + \gamma_2 L(\psi)) = \gamma_1 D^{\beta}_{M,\chi}(K(\chi)) + \gamma_2 D^{\beta}_{M,\chi}(L(\chi))$,

ii) $D^{\beta}_{M,\chi}(K(\chi) L(\chi)) = K(\chi) D^{\beta}_{M,\chi}(L(\chi)) + L(\chi) D^{\beta}_{M,\chi}(K(\chi))$.

iii) $D^{\beta}_{M,\chi}\left(\frac{K(\chi)}{L(\chi)}\right) = \frac{K(\psi) D^{\beta}_{M,\chi}(L(\chi)) - L(\chi) D^{\beta}_{M,\chi}(K(\chi))}{L^{2}(\chi)}$.

iv) $D^{\beta}_{M,\chi}(p) = 0$, for any constant p.

v) $D^{\beta}_{M,\chi} K(\chi) = \frac{\chi^{1-\beta}}{\Gamma(\delta + 1)} \frac{dK}{d\delta}$.

Conformable Derivative (CD):

The CD for the function $\tau: [q, \infty) \to \Re$ of order $\beta \in (0, 1]$ is defined as below:

$$D^{\beta}_{C,t}\Theta(t) = \lim_{\varpi \to 0} \frac{\Theta\left(t + \varpi (t)^{1-\beta}\right) - \varpi(t)}{\varpi}, \; t > 0.$$

For any affirmative value of t, the limit specified in the above equation shows the presence of the β-CD of Θ. Presume $0 < \beta \leq 1$, and $\Theta(t), f(t)$ symbolize β-CD functions. The CD retains numerous imperative possessions as outlined below:

i) $D^{\beta}_{t}(p) = 0$, where p =constant.

ii) $D^{\beta}_{t}(t^{\mu}) = \mu t^{\mu - \chi}$, for all $\mu \in R$.

iii) $D^{\beta}_{t}(a_1\Theta(t) + a_2 f(t)) = a_1 D^{\beta}_{t}\Theta(t) + a_2 D^{\beta}_{t} f(t), \forall a_1, a_2 \in R$.

iv) $D^{\beta}_{t}(\Theta(t) f(t)) = \Theta(t) D^{\beta}_{t} f(t) + f(t) D^{\beta}_{t} h(t)$.

v) $D^{\beta}_{t}\left(\frac{\Theta(t)}{f(t)}\right) = \frac{f(t) D^{\beta}_{t}\Theta(t) - \Theta(t) D^{\beta}_{t} f(t)}{f(t)^{2}}$.

vi) If Θ is differential, then $D^{\beta}_{t}(\Theta(t)) = t^{1-\beta} \frac{d\Theta(t)}{dt}$.

Furthermore, the possessions and formulas associated with the conformable derivatives are treated completely from a reference perspective [46].

3 The Proposed Method

Consider the nonlinear partial differential equation (NLPDE) as follows:

$$\Omega\left(\Psi, \Psi_x, \Psi_y, \Psi_t, \Psi_{xx}, \Psi_{yy}, \Psi_{tt}, \ldots\right) = 0, \tag{1}$$

where $\Psi = \Psi(x, y, t)$ is an unidentified function, Ω is a polynomial in Ψ and its partial derivatives. The key stages of the projected scheme are:

Stage 1: Assume the wave variable $\eta = x + y - \omega\ \ t$, where ω symbolizes the wave speed, converts the Eq. (1) to the subsequent nonlinear ordinary differential equation (ODE):

$$\Xi\left(\Psi, \omega\Psi', \Psi'', \Psi', \omega^2\Psi'', -\omega\ \ \Psi'', \ldots\right) = 0. \tag{2}$$

Stage 2: Presume the trial solution of Eq. (2) can be articulated in a power series with the subsequent format:

$$\Psi(\eta) = \sum_{j=-n}^{n} \varphi_j \left(\Xi(\eta)\right)^i, \tag{3}$$

where $\Xi(\eta) = H + \frac{G'(\eta)}{G^2(\eta)}$, and $\varphi_j\,(j = \pm 1, \ldots, \pm n)$ and H are constants. By bearing in mind the homogeneous balance between the highest-order nonlinear term and highest-order derivative in Eq. (2), the positive integer n can be assessed. It is presumed that $\left(G'/G^2\right)$ satisfies the subsequent Riccati equation:

$$\left(G'/G^2\right)' = \vartheta_1 + \vartheta_2\left(G'/G^2\right)^2 + \vartheta_3\left(G'/G^2\right). \tag{4}$$

The possible solutions to Eq. (4) are:

$$\frac{G'}{G^2} = \begin{cases} \dfrac{\sqrt{\vartheta_1\vartheta_2}\left(\theta_1\cos\left(\sqrt{\vartheta_1\vartheta_2}\eta\right) + \theta_2\sin\left(\sqrt{\vartheta_1\vartheta_2}\eta\right)\right)}{\vartheta_1\left(\theta_2\cos\left(\sqrt{\vartheta_1\vartheta_2}\eta\right) - \theta_1\sin\left(\sqrt{\vartheta_1\vartheta_2}\eta\right)\right)} & \vartheta_1\vartheta_2 > 0, \vartheta_3 = 0, \\ \dfrac{-\sqrt{|\vartheta_1\vartheta_2|}\left(\theta_1\sinh\left(2\sqrt{|\vartheta_1\vartheta_2|}\eta\right) + \theta_1\cosh\left(2\sqrt{|\vartheta_1\vartheta_2|}\eta\right) + \theta_2\right)}{\vartheta_1\left(\theta_1\sinh\left(2\sqrt{|\vartheta_1\vartheta_2|}\eta\right) + \theta_1\cosh\left(2\sqrt{|\vartheta_1\vartheta_2|}\eta\right) - \theta_2\right)} & \vartheta_1\vartheta_2 < 0, \vartheta_3 = 0, \\ \dfrac{-\theta_1}{\vartheta_2\left(\theta_1\eta + Q\right)} & \vartheta_1 = 0, \vartheta_2 \neq 0, \vartheta_3 = 0, \\ \dfrac{-\vartheta_3}{2\vartheta_2} - \dfrac{\sqrt{\Delta}\left(\theta_1\cosh\left(\frac{\sqrt{\Delta}}{2}\eta\right) + \theta_2\sinh\left(\frac{\sqrt{\Delta}}{2}\eta\right)\right)}{2\vartheta_2\left(\theta_2\cosh\left(\frac{\sqrt{\Delta}}{2}\eta\right) + \theta_1\sinh\left(\frac{\sqrt{\Delta}}{2}\eta\right)\right)} & \vartheta_3 \neq 0, \Delta \geq 0, \\ \dfrac{-\vartheta_3}{2\vartheta_2} - \dfrac{\sqrt{-\Delta}\left(\theta_1\cos\left(\frac{\sqrt{-\Delta}}{2}\eta\right) - \theta_2\sin\left(\frac{\sqrt{-\Delta}}{2}\eta\right)\right)}{2\vartheta_2\left(\theta_1\sin\left(\frac{\sqrt{-\Delta}}{2}\eta\right) + \theta_2\cos\left(\frac{\sqrt{-\Delta}}{2}\eta\right)\right)} & \vartheta_3 \neq 0, \Delta < 0, \end{cases} \tag{5}$$

where θ_1 and θ_2 are capricious constants and $\Delta = \vartheta_3^2 - 4\vartheta_1\vartheta_2$.

Stage 3: To get the arithmetical system for ω and $\varphi_j\,(j = \pm 1, \ldots, \pm n)$, we need to set the coefficients from $(\Xi)^j$ to zero, then substitute the Eqs. (3) and (4) to Eq. (2).

Step 4: Solving the acquired arithmetical system by via computational software Maple 18 to find the values of ω and $\varphi_j\,(j = \pm 1, \ldots, \pm n)$, placing the value of Ξ into Eqs. (3) from (5) to acquire the precise solutions of Eq. (2).

4 The Method's Application

In this segment, we examine the $(2+1)$ dimensional NLWKB [47]:

$$U_{tt} + n\,U_{ty} - lU_{xx}^2 - U_{xx} - m\,U_{xxxx} + \frac{1}{4}n^2 U_{yy} = 0, \tag{6}$$

where $m,\ n, l$ are non-zero parameters. In terms of β-derivative, this model can be articulated as:

$$D_{\beta,t}^{\gamma}\,U_{tt} + n\,D_{\beta,t}^{\gamma}\,U_{ty} - lU_{xx}^2 - U_{xx} - m\,U_{xxxx} + \frac{1}{4}n^2 U_{yy} = 0, \tag{7}$$

where $D_{\beta,t}^{\gamma}$ is β-derivative of $w(x, y, t)$ and γ displays the fractional constraint such that $0 \leq \gamma \leq 1$.

In β-derivative, η shows the wave transformation that converts the original PDE into an ODE, allowing us to discover exact traveling wave solutions and proceeds the subsequent form:

$$U\,(x, y, t) = U\,(\eta)\ ,\ \eta = k\left(x + y - v\frac{\left(t + \dfrac{1}{\Gamma\,(\beta)}\right)^{\beta}}{\beta}\right),\ \ k, v \neq 0. \tag{8}$$

The model is expressed for M-truncated derivative in the following way:

$$D_{M,t}^{\gamma}\,U_{tt} + n\,D_{M,t}^{\gamma}\,U_{ty} - l\,U_{xx}^2 - U_{xx} - m\,U_{xxxx} + \frac{1}{4}n^2 U_{yy} = 0, \tag{9}$$

where $D_{M,t}^{\gamma}$ is the M-truncated derivative, while γ is the fractional order derivative. In M-Truncated derivative, the travelling wave constraint η takes the subsequent form:

$$w\ (x, y, t) = w\,(\eta)\ ,\ \eta = k\left(x + y + v\frac{\Gamma\,(\gamma+1)}{\beta}t^{\beta}\right). \tag{10}$$

The model is expressed as a conformable derivative in the following way:

$$D_{C,t}^{\gamma}\,w_{tt} + n\,D_{C,t}^{\gamma}\,w_{ty} - l\,w_{xx}^2 - w_{xx} - m\,w_{xxxx} + \frac{1}{4}n^2 w_{yy} = 0. \tag{11}$$

In Eq. (11), $D_{C,t}^{\gamma}$ is conformable derivative, while γ is the fractional order derivative.

In CD, the travelling wave constraint η proceeds in the following form:

$$w\ (x, y, t) = w\,(\eta)\ ,\ \eta = k\left(x + y + \frac{v}{\beta}t^{\beta}\right), \tag{12}$$

transforms Eqs. (7), (9) and (11) into ordinary differential equations using their analogous wave conversions mentioned in Eqs. (8), (10) and (12), we get:

$$-4k^2m\,w^{(iv)}+\left(4\nu^2-4\nu\,n+n^2-4\right)w''-8l\left(w\,w''+(w')^2\right)=0. \tag{13}$$

Integrating Eq. (13) twofold with respect to η and setting the constant of integration to zero, we acquire the subsequent ordinary differential equation:

$$4k^2m\,w''+4lw^2-\left(4\nu^2-4\nu\,n+n^2-4\right)w=0. \tag{14}$$

The balance number $N=2$ is obtained by equating the highest-order linear term w'' with the highest-order nonlinear term w^2 in the Eq. (14) by using the balancing principle. This helps to develop a suitable solution, confirming that the obtained solitons satisfy the governing equation. The Eq. (3) can be written in the following form by using $N=2$ as:

$$w(\eta)=\varphi_0+\varphi_1(\Xi)+\varphi_2(\Xi)^2+\varphi_{-1}(\Xi)^{-1}+\varphi_{-2}(\Xi)^{-2}, \tag{15}$$

where $G=G(\eta)$, and $\varphi_0,\varphi_1,\varphi_2,\varphi_{-1},\varphi_{-2}$ are the unidentified quantities to be gritty. Putting Eq. (15) together with Eqs. (4) into (14), then equating the quantities of $w(\eta)$ to zero, we acquire a structure of nonlinear equations. Unravelling the acquired structure with Maple 18, we find the subsequent solution sets.

Set 1:

$$\varphi_0=-\frac{k^2m\Delta}{l},\varphi_2=-\frac{6\vartheta_2^2k^2m}{l},\varphi_{-2}=-\frac{3mk^2\Delta^2}{8l\vartheta_2^2},H=\frac{\vartheta_3}{2\vartheta_2},\nu=\frac{1}{2}n+\sqrt{1-4mk^2\Delta},\ \varphi_1=\varphi_{-1}=0. \tag{16}$$

By inserting the obtained values of constants from Eq. (16) along with the values from Eqs. (5) into (15), we derive the subsequent results for Set 1:

$$w_{11}(\eta)=-\frac{k^2m\Delta}{l}-\frac{6\vartheta_2^2k^2m}{l}\left(\frac{\vartheta_3}{2\vartheta_2}+\frac{\sqrt{\vartheta_1\vartheta_2}\left(\theta_1\cos\left(\sqrt{\vartheta_1\vartheta_2}\eta\right)+\theta_2\sin\left(\sqrt{\vartheta_1\vartheta_2}\eta\right)\right)}{\vartheta_1\left(\theta_2\cos\left(\sqrt{\vartheta_1\vartheta_2}\eta\right)-\theta_1\sin\left(\sqrt{\vartheta_1\vartheta_2}\eta\right)\right)}\right)^2$$
$$-\frac{3mk^2\Delta^2}{8l\vartheta_2^2}\left(\frac{\vartheta_3}{2\vartheta_2}+\frac{\sqrt{\vartheta_1\vartheta_2}\left(\theta_1\cos\left(\sqrt{\vartheta_1\vartheta_2}\eta\right)+\theta_2\sin\left(\sqrt{\vartheta_1\vartheta_2}\eta\right)\right)}{\vartheta_1\left(\theta_2\cos\left(\sqrt{\vartheta_1\vartheta_2}\eta\right)-\theta_1\sin\left(\sqrt{\vartheta_1\vartheta_2}\eta\right)\right)}\right)^{-2}, \tag{17}$$

$$w_{12}(\eta)=-\frac{k^2m\Delta}{l}-\frac{6\vartheta_2^2k^2m}{l}\left(\frac{\vartheta_3}{2\vartheta_2}-\frac{\sqrt{|\vartheta_1\vartheta_2|}\left(\theta_1\sin h\left(2\sqrt{|\vartheta_1\vartheta_2|}\eta\right)+\theta_1\cos h\left(2\sqrt{|\vartheta_1\vartheta_2|}\eta\right)+\theta_2\right)}{\vartheta_1\left(\theta_1\sin h\left(2\sqrt{|\vartheta_1\vartheta_2|}\eta\right)+\theta_1\cos h\left(2\sqrt{|\vartheta_1\vartheta_2|}\eta\right)-\theta_2\right)}\right)^2$$
$$-\frac{3mk^2\Delta^2}{8l\vartheta_2^2}\left(\frac{\vartheta_3}{2\vartheta_2}-\frac{\sqrt{|\vartheta_1\vartheta_2|}\left(\theta_1\sin h\left(2\sqrt{|\vartheta_1\vartheta_2|}\eta\right)+\theta_1\cos h\left(2\sqrt{|\vartheta_1\vartheta_2|}\eta\right)+\theta_2\right)}{\vartheta_1\left(\theta_1\sin h\left(2\sqrt{|\vartheta_1\vartheta_2|}\eta\right)+\theta_1\cos h\left(2\sqrt{|\vartheta_1\vartheta_2|}\eta\right)-\theta_2\right)}\right)^{-2}, \tag{18}$$

$$w_{13}(\eta)=-\frac{k^2m\Delta}{l}-\frac{6\vartheta_2^2k^2m}{l}\left(\frac{\vartheta_3}{2\vartheta_2}-\frac{\theta_1}{\vartheta_2\left(\theta_1\eta+Q\right)}\right)^2-\frac{3mk^2\Delta^2}{8l\vartheta_2^2}\left(\frac{\vartheta_3}{2\vartheta_2}-\frac{\theta_1}{\vartheta_2\left(\theta_1\eta+Q\right)}\right)^{-2}, \tag{19}$$

$$w_{14}(\eta) = -\frac{k^2 m\Delta}{l} + \frac{6\vartheta_2^2 k^2 m}{l}\left(\frac{\sqrt{\Delta}\left(\theta_1 \cosh\left(\frac{\sqrt{\Delta}}{2}\eta\right) + \theta_2 \sinh\left(\frac{\sqrt{\Delta}}{2}\eta\right)\right)}{2\vartheta_2\left(\theta_2 \cosh\left(\frac{\sqrt{\Delta}}{2}\eta\right) + \theta_1 \sinh\left(\frac{\sqrt{\Delta}}{2}\eta\right)\right)}\right)^2 + \frac{3mk^2\Delta^2}{8l\vartheta_2^2}\left(\frac{\sqrt{\Delta}\left(\theta_1 \cosh\left(\frac{\sqrt{\Delta}}{2}\eta\right) + \theta_2 \sinh\left(\frac{\sqrt{\Delta}}{2}\eta\right)\right)}{2\vartheta_2\left(\theta_2 \cosh\left(\frac{\sqrt{\Delta}}{2}\eta\right) + \theta_1 \sinh\left(\frac{\sqrt{\Delta}}{2}\eta\right)\right)}\right)^{-2}, \tag{20}$$

$$w_{15}(\zeta) = -\frac{k^2 m\Delta}{l} + \frac{6\vartheta_2^2 k^2 m}{l}\left(\frac{\sqrt{-\Delta}\left(\theta_1 \cos\left(\frac{\sqrt{-\Delta}}{2}\eta\right) - \theta_2 \sin\left(\frac{\sqrt{-\Delta}}{2}\eta\right)\right)}{2\vartheta_2\left(\theta_1 \sin\left(\frac{\sqrt{-\Delta}}{2}\eta\right) + \theta_2 \cos\left(\frac{\sqrt{-\Delta}}{2}\eta\right)\right)}\right)^2 + \frac{3mk^2\Delta^2}{8l\vartheta_2^2}\left(\frac{\sqrt{-\Delta}\left(\theta_1 \cos\left(\frac{\sqrt{-\Delta}}{2}\eta\right) - \theta_2 \sin\left(\frac{\sqrt{-\Delta}}{2}\eta\right)\right)}{2\vartheta_2\left(\theta_1 \sin\left(\frac{\sqrt{-\Delta}}{2}\eta\right) + \theta_2 \cos\left(\frac{\sqrt{-\Delta}}{2}\eta\right)\right)}\right)^{-2}. \tag{21}$$

Set 2:

$$H = \frac{\vartheta_3}{2\vartheta_2}, \nu = \frac{1}{2}n + \sqrt{1+4mk^2\Delta}, \varphi_0 = \frac{3k^2 m\Delta}{l}, \varphi_1 = 0, \varphi_2 = -\frac{6\vartheta_2^2 k^2 m}{l}, \varphi_{-1} = 0, \varphi_{-2} = -\frac{3mk^2\Delta^2}{8l\vartheta_2^2}. \tag{22}$$

By inserting the obtained values of constants from Eq. (22) along with the values from Eqs. (5) into (15), we derive the subsequent solutions for Set 2:

$$w_{21}(\eta) = \frac{3k^2 m\Delta}{l} - \frac{6\vartheta_2^2 k^2 m}{l}\left(\frac{\vartheta_3}{2\vartheta_2} + \frac{\sqrt{\vartheta_1\vartheta_2}\left(\theta_1 \cos\left(\sqrt{\vartheta_1\vartheta_2}\eta\right) + \theta_2 \sin\left(\sqrt{\vartheta_1\vartheta_2}\eta\right)\right)}{\vartheta_1\left(\theta_2 \cos\left(\sqrt{\vartheta_1\vartheta_2}\eta\right) - \theta_1 \sin\left(\sqrt{\vartheta_1\vartheta_2}\eta\right)\right)}\right)^2 - \frac{3mk^2\Delta^2}{8l\vartheta_2^2}\left(\frac{\vartheta_3}{2\vartheta_2} + \frac{\sqrt{\vartheta_1\vartheta_2}\left(\theta_1 \cos\left(\sqrt{\vartheta_1\vartheta_2}\eta\right) + \theta_2 \sin\left(\sqrt{\vartheta_1\vartheta_2}\eta\right)\right)}{\vartheta_1\left(\theta_2 \cos\left(\sqrt{\vartheta_1\vartheta_2}\eta\right) - \theta_1 \sin\left(\sqrt{\vartheta_1\vartheta_2}\eta\right)\right)}\right)^{-2}, \tag{23}$$

$$w_{22}(\eta) = \frac{3k^2 m\Delta}{l} - \frac{6\vartheta_2^2 k^2 m}{l}\left(\frac{\vartheta_3}{2\vartheta_2} - \frac{\sqrt{|\vartheta_1\vartheta_2|}\left(\theta_1 \sinh\left(2\sqrt{|\vartheta_1\vartheta_2|}\eta\right) + \theta_1 \cosh\left(2\sqrt{|\vartheta_1\vartheta_2|}\eta\right) + \theta_2\right)}{\vartheta_1\left(\theta_1 \sinh\left(2\sqrt{|\vartheta_1\vartheta_2|}\eta\right) + \theta_1 \cosh\left(2\sqrt{|\vartheta_1\vartheta_2|}\eta\right) - \theta_2\right)}\right)^2 - \frac{3mk^2\Delta^2}{8l\vartheta_2^2}\left(\frac{\vartheta_3}{2\vartheta_2} - \frac{\sqrt{|\vartheta_1\vartheta_2|}\left(\theta_1 \sinh\left(2\sqrt{|\vartheta_1\vartheta_2|}\eta\right) + \theta_1 \cosh\left(2\sqrt{|\vartheta_1\vartheta_2|}\eta\right) + \theta_2\right)}{\vartheta_1\left(\theta_1 \sinh\left(2\sqrt{|\vartheta_1\vartheta_2|}\eta\right) + \theta_1 \cosh\left(2\sqrt{|\vartheta_1\vartheta_2|}\eta\right) - \theta_2\right)}\right)^{-2}, \tag{24}$$

$$w_{23}(\eta) = \frac{3k^2 m\Delta}{l} - \frac{6\vartheta_2^2 k^2 m}{l}\left(\frac{\vartheta_3}{2\vartheta_2} - \frac{\theta_1}{\vartheta_2(\theta_1\eta + \theta_2)}\right)^2 - \frac{3mk^2\Delta^2}{8l\vartheta_2^2}\left(\frac{\vartheta_3}{2\vartheta_2} - \frac{\theta_1}{\vartheta_2(\theta_1\eta + \theta_2)}\right)^{-2}, \tag{25}$$

$$w_{24}(\eta) = \frac{3k^2 m\Delta}{l} + \frac{6\vartheta_2^2 k^2 m}{l}\left(\frac{\sqrt{\Delta}\left(\theta_1 \cosh\left(\frac{\sqrt{\Delta}}{2}\eta\right) + \theta_2 \sinh\left(\frac{\sqrt{\Delta}}{2}\eta\right)\right)}{2\vartheta_2\left(\theta_2 \cosh\left(\frac{\sqrt{\Delta}}{2}\eta\right) + \theta_1 \sinh\left(\frac{\sqrt{\Delta}}{2}\eta\right)\right)}\right)^2 + \frac{3mk^2\Delta^2}{8l\vartheta_2^2}\left(\frac{\sqrt{\Delta}\left(\theta_1 \cosh\left(\frac{\sqrt{\Delta}}{2}\eta\right) + \theta_2 \sinh\left(\frac{\sqrt{\Delta}}{2}\eta\right)\right)}{2\vartheta_2\left(\theta_2 \cosh\left(\frac{\sqrt{\Delta}}{2}\eta\right) + \theta_1 \sinh\left(\frac{\sqrt{\Delta}}{2}\eta\right)\right)}\right)^{-2}, \tag{26}$$

$$w_{25}(\eta)=\frac{3k^2m\Delta}{l}+\frac{6\vartheta_2^2k^2m}{l}\left(\frac{\sqrt{-\Delta}\left(\theta_1\cos\left(\frac{\sqrt{-\Delta}}{2}\eta\right)-\theta_2\sin\left(\frac{\sqrt{-\Delta}}{2}\eta\right)\right)}{2\vartheta_2\left(\theta_1\sin\left(\frac{\sqrt{-\Delta}}{2}\eta\right)+\theta_2\cos\left(\frac{\sqrt{-\Delta}}{2}\eta\right)\right)}\right)^2$$
$$+\frac{3mk^2\Delta^2}{8l\vartheta_2^2}\left(\frac{\sqrt{-\Delta}\left(\theta_1\cos\left(\frac{\sqrt{-\Delta}}{2}\eta\right)-\theta_2\sin\left(\frac{\sqrt{-\Delta}}{2}\eta\right)\right)}{2\vartheta_2\left(\theta_1\sin\left(\frac{\sqrt{-\Delta}}{2}\eta\right)+\theta_2\cos\left(\frac{\sqrt{-\Delta}}{2}\eta\right)\right)}\right)^{-2}. \tag{27}$$

Set 3:

$$\varphi_0=-\frac{6k^2m\vartheta_2\left(\vartheta_2H^2-H\vartheta_3+\vartheta_1\right)}{l},\ \varphi_1=\frac{6k^2m\vartheta_2\left(2H\vartheta_2-\vartheta_3\right)}{l},\ \varphi_2=-\frac{6\vartheta_2^2k^2m}{l},$$
$$\nu=\frac{1}{2}n+\sqrt{1+mk^2\Delta},\phi_{-1}=0,\phi_{-2}=0,H=H. \tag{28}$$

By inserting the obtained values of constants from Eq. (28) along with the values from Eqs. (5) into (15), we derive the subsequent solutions for Set 3:

$$w_{31}(\eta)=\frac{6k^2m\vartheta_2\left(2H\vartheta_2-\vartheta_3\right)}{l}\left(H+\frac{\sqrt{\vartheta_1\vartheta_2}\left(\theta_1\cos\left(\sqrt{\vartheta_1\vartheta_2}\eta\right)+\theta_2\sin\left(\sqrt{\vartheta_1\vartheta_2}\eta\right)\right)}{\vartheta_1\left(\theta_2\cos\left(\sqrt{\vartheta_1\vartheta_2}\eta\right)-\theta_1\sin\left(\sqrt{\vartheta_1\vartheta_2}\eta\right)\right)}\right)$$
$$-\frac{6\vartheta_2^2k^2m}{l}\left(H+\frac{\sqrt{\vartheta_1\vartheta_2}\left(\theta_1\cos\left(\sqrt{\vartheta_1\vartheta_2}\eta\right)+\theta_2\sin\left(\sqrt{\vartheta_1\vartheta_2}\eta\right)\right)}{\vartheta_1\left(\theta_2\cos\left(\sqrt{\vartheta_1\vartheta_2}\eta\right)-\theta_1\sin\left(\sqrt{\vartheta_1\vartheta_2}\eta\right)\right)}\right)^2-\frac{6k^2m\vartheta_2\left(\vartheta_2H^2-H\vartheta_3+\vartheta_1\right)}{l}, \tag{29}$$

$$w_{32}(\eta)=\frac{6k^2m\vartheta_2\left(2H\vartheta_2-\vartheta_3\right)}{l}\left(H-\frac{\sqrt{|\vartheta_1\vartheta_2|}\left(\theta_1\sinh\left(2\sqrt{|\vartheta_1\vartheta_2|}\eta\right)+\theta_1\cosh\left(2\sqrt{|\vartheta_1\vartheta_2|}\eta\right)+\theta_2\right)}{\vartheta_1\left(\theta_1\sinh\left(2\sqrt{|\vartheta_1\vartheta_2|}\eta\right)+\theta_1\cosh\left(2\sqrt{|\vartheta_1\vartheta_2|}\eta\right)-\theta_2\right)}\right)$$
$$-\frac{6\vartheta_2^2k^2m}{l}\left(H-\frac{\sqrt{|\vartheta_1\vartheta_2|}\left(\theta_1\sinh\left(2\sqrt{|\vartheta_1\vartheta_2|}\eta\right)+\theta_1\cosh\left(2\sqrt{|\vartheta_1\vartheta_2|}\eta\right)+\theta_2\right)}{\vartheta_1\left(\theta_1\sinh\left(2\sqrt{|\vartheta_1\vartheta_2|}\eta\right)+\theta_1\cosh\left(2\sqrt{|\vartheta_1\vartheta_2|}\eta\right)-\theta_2\right)}\right)^2$$
$$-\frac{6k^2m\vartheta_2\left(\vartheta_2H^2-H\vartheta_3+\vartheta_1\right)}{l}, \tag{30}$$

$$w_{33}(\eta)=\frac{6k^2m\vartheta_2\left(2H\vartheta_2-\vartheta_3\right)}{l}\left(H-\frac{\theta_1}{\vartheta_2\left(\theta_1\eta+Q\right)}\right)-\frac{6\vartheta_2^2k^2m}{l}\left(H-\frac{\theta_1}{\vartheta_2\left(\theta_1\eta+Q\right)}\right)^2$$
$$-\frac{6k^2m\vartheta_2\left(\vartheta_2H^2-H\vartheta_3+\vartheta_1\right)}{l}, \tag{31}$$

$$w_{34}(\eta)=\frac{6k^2m\vartheta_2\left(2H\vartheta_2-\vartheta_3\right)}{l}\left(H-\frac{\vartheta_3}{2\vartheta_2}-\frac{\sqrt{\Delta}\left(\theta_1\cosh\left(\frac{\sqrt{\Delta}}{2}\eta\right)+\theta_2\sinh\left(\frac{\sqrt{\Delta}}{2}\eta\right)\right)}{2\vartheta_2\left(\theta_2\cosh\left(\frac{\sqrt{\Delta}}{2}\eta\right)+\theta_1\sinh\left(\frac{\sqrt{\Delta}}{2}\eta\right)\right)}\right)$$
$$-\frac{6\vartheta_2^2k^2m}{l}\left(H-\frac{\vartheta_3}{2\vartheta_2}-\frac{\sqrt{\Delta}\left(\theta_1\cosh\left(\frac{\sqrt{\Delta}}{2}\eta\right)+\theta_2\sinh\left(\frac{\sqrt{\Delta}}{2}\eta\right)\right)}{2\vartheta_2\left(\theta_2\cosh\left(\frac{\sqrt{\Delta}}{2}\eta\right)+\theta_1\sinh\left(\frac{\sqrt{\Delta}}{2}\eta\right)\right)}\right)^2$$
$$-\frac{6k^2m\vartheta_2\left(\vartheta_2H^2-H\vartheta_3+\vartheta_1\right)}{l}, \tag{32}$$

$$w_{35}(\eta) = \frac{6k^2m\vartheta_2(2H\vartheta_2-\vartheta_3)}{l}\left(H-\frac{\vartheta_3}{2\vartheta_2}-\frac{\sqrt{-\Delta}\left(\theta_1\cos\left(\frac{\sqrt{-\Delta}}{2}\eta\right)-\theta_2\sin\left(\frac{\sqrt{-\Delta}}{2}\eta\right)\right)}{2\vartheta_2\left(\theta_1\sin\left(\frac{\sqrt{-\Delta}}{2}\eta\right)+\theta_2\cos\left(\frac{\sqrt{-\Delta}}{2}\eta\right)\right)}\right)$$
$$-\frac{6\vartheta_2^2k^2m}{l}\left(H-\frac{\vartheta_3}{2\vartheta_2}-\frac{\sqrt{-\Delta}\left(\theta_1\cos\left(\frac{\sqrt{-\Delta}}{2}\eta\right)-\theta_2\sin\left(\frac{\sqrt{-\Delta}}{2}\eta\right)\right)}{2\vartheta_2\left(\theta_1\sin\left(\frac{\sqrt{-\Delta}}{2}\eta\right)+\theta_2\cos\left(\frac{\sqrt{-\Delta}}{2}\eta\right)\right)}\right)^2$$
$$-\frac{6k^2m\vartheta_2\left(\vartheta_2H^2-H\vartheta_3+\vartheta_1\right)}{l}. \tag{33}$$

Set 4:

$$H=H,\nu=\frac{1}{2}n+\sqrt{1-mk^2\Delta},\ \phi_0=-\frac{k^2m\left(6\vartheta_2^2H^2-6\vartheta_2H\vartheta_3+2\vartheta_1\vartheta_2+\vartheta_3^2\right)}{l},$$
$$\phi_1=\frac{6k^2m\vartheta_2(2H\vartheta_2-\vartheta_3)}{l},\ \phi_2=-\frac{6\vartheta_2^2k^2m}{l},\phi_{-1}=0,\phi_{-2}=0. \tag{34}$$

By inserting the obtained values of constants from Eq. (34) along with the values from Eqs. (5) into (15), we derive the subsequent solutions for Set 4:

$$w_{41}(\eta) = -\frac{k^2m\left(6\vartheta_2^2H^2-6\vartheta_2H\vartheta_3+2\vartheta_1\vartheta_2+\vartheta_3^2\right)}{l}$$
$$+\frac{6k^2m\vartheta_2(2H\vartheta_2-\vartheta_3)}{l}\left(H+\frac{\sqrt{\vartheta_1\vartheta_2}\left(\theta_1\cos\left(\sqrt{\vartheta_1\vartheta_2}\eta\right)+\theta_2\sin\left(\sqrt{\vartheta_1\vartheta_2}\eta\right)\right)}{\vartheta_1\left(\theta_2\cos\left(\sqrt{\vartheta_1\vartheta_2}\eta\right)-\theta_1\sin\left(\sqrt{\vartheta_1\vartheta_2}\eta\right)\right)}\right)$$
$$-\frac{6\vartheta_2^2k^2m}{l}\left(H+\frac{\sqrt{\vartheta_1\vartheta_2}\left(\theta_1\cos\left(\sqrt{\vartheta_1\vartheta_2}\eta\right)+\theta_2\sin\left(\sqrt{\vartheta_1\vartheta_2}\eta\right)\right)}{\vartheta_1\left(\theta_2\cos\left(\sqrt{\vartheta_1\vartheta_2}\eta\right)-\theta_1\sin\left(\sqrt{\vartheta_1\vartheta_2}\eta\right)\right)}\right)^2, \tag{35}$$

$$w_{42}(\eta) = -\frac{k^2m\left(6\vartheta_2^2H^2-6\vartheta_2H\vartheta_3+2\vartheta_1\vartheta_2+\vartheta_3^2\right)}{l}$$
$$+\frac{6k^2m\vartheta_2(2H\vartheta_2-\vartheta_3)}{l}\left(H-\frac{\sqrt{|\vartheta_1\vartheta_2|}\left(\theta_1\sinh\left(2\sqrt{|\vartheta_1\vartheta_2|}\eta\right)+\theta_1\cosh\left(2\sqrt{|\vartheta_1\vartheta_2|}\eta\right)+\theta_2\right)}{\vartheta_1\left(\theta_1\sinh\left(2\sqrt{|\vartheta_1\vartheta_2|}\eta\right)+\theta_1\cosh\left(2\sqrt{|\vartheta_1\vartheta_2|}\eta\right)-\theta_2\right)}\right)$$
$$-\frac{6\vartheta_2^2k^2m}{l}\left(H-\frac{\sqrt{|\vartheta_1\vartheta_2|}\left(\theta_1\sinh\left(2\sqrt{|\vartheta_1\vartheta_2|}\eta\right)+\theta_1\cosh\left(2\sqrt{|\vartheta_1\vartheta_2|}\eta\right)+\theta_2\right)}{\vartheta_1\left(\theta_1\sinh\left(2\sqrt{|\vartheta_1\vartheta_2|}\eta\right)+\theta_1\cosh\left(2\sqrt{|\vartheta_1\vartheta_2|}\eta\right)-\theta_2\right)}\right)^2, \tag{36}$$

$$w_{43}(\eta) = \frac{6k^2m\vartheta_2(2H\vartheta_2-\vartheta_3)}{l}\left(H-\frac{\theta_1}{\vartheta_2(\theta_1\eta+Q)}\right)-\frac{6\vartheta_2^2k^2m}{l}\left(H-\frac{\theta_1}{\vartheta_2(\theta_1\eta+Q)}\right)^2$$
$$-\frac{k^2m\left(6\vartheta_2^2H^2-6\vartheta_2H\vartheta_3+2\vartheta_1\vartheta_2+\vartheta_3^2\right)}{l}, \tag{37}$$

$$w_{44}(\eta) = -\frac{k^2 m\left(6\vartheta_2^2 H^2 - 6\vartheta_2 H\vartheta_3 + 2\vartheta_1\vartheta_2 + \vartheta_3^2\right)}{l} + \frac{6k^2 m\vartheta_2\left(2H\vartheta_2 - \vartheta_3\right)}{l}\left(H - \frac{\vartheta_3}{2\vartheta_2} - \frac{\sqrt{\Delta}\left(\theta_1 \cosh\left(\frac{\sqrt{\Delta}}{2}\eta\right) + \theta_2 \sinh\left(\frac{\sqrt{\Delta}}{2}\eta\right)\right)}{2\vartheta_2\left(\theta_2 \cosh\left(\frac{\sqrt{\Delta}}{2}\eta\right) + \theta_1 \sinh\left(\frac{\sqrt{\Delta}}{2}\eta\right)\right)}\right) - \frac{6\vartheta_2^2 k^2 m}{l}\left(H - \frac{\vartheta_3}{2\vartheta_2} - \frac{\sqrt{\Delta}\left(\theta_1 \cosh\left(\frac{\sqrt{\Delta}}{2}\eta\right) + \theta_2 \sinh\left(\frac{\sqrt{\Delta}}{2}\eta\right)\right)}{2\vartheta_2\left(\theta_2 \cosh\left(\frac{\sqrt{\Delta}}{2}\eta\right) + \theta_1 \sinh\left(\frac{\sqrt{\Delta}}{2}\eta\right)\right)}\right)^2, \tag{38}$$

$$w_{45}(\eta) = -\frac{k^2 m\left(6\vartheta_2^2 H^2 - 6\vartheta_2 H\vartheta_3 + 2\vartheta_1\vartheta_2 + \vartheta_3^2\right)}{l} + \frac{6k^2 m\vartheta_2\left(2H\vartheta_2 - \vartheta_3\right)}{l}\left(H - \frac{\vartheta_3}{2\vartheta_2} - \frac{\sqrt{-\Delta}\left(\theta_1 \cos\left(\frac{\sqrt{-\Delta}}{2}\eta\right) - \theta_2 \sin\left(\frac{\sqrt{-\Delta}}{2}\eta\right)\right)}{2\vartheta_2\left(\theta_1 \sin\left(\frac{\sqrt{-\Delta}}{2}\eta\right) + \theta_2 \cos\left(\frac{\sqrt{-\Delta}}{2}\eta\right)\right)}\right) - \frac{6\vartheta_2^2 k^2 m}{l}\left(H - \frac{\vartheta_3}{2\vartheta_2} - \frac{\sqrt{-\Delta}\left(\theta_1 \cos\left(\frac{\sqrt{-\Delta}}{2}\eta\right) - \theta_2 \sin\left(\frac{\sqrt{-\Delta}}{2}\eta\right)\right)}{2\vartheta_2\left(\theta_1 \sin\left(\frac{\sqrt{-\Delta}}{2}\eta\right) + \theta_2 \cos\left(\frac{\sqrt{-\Delta}}{2}\eta\right)\right)}\right)^2. \tag{39}$$

Remark 1: If we put $H = 0, \vartheta_1 = \upsilon, \vartheta_2 = \Lambda, \vartheta_3 = Y, \theta_1 = \phi_1, \theta_2 = \phi_2, w = \vartheta, l = x_1, m = x_2, n = x_3, k = u$, and $\eta = \psi$, then our solution Eqs. (35)–(39) exactly coincide with the solution Eqs. (4.38)–(4.42) of Saboor et al. [44].

Set 5:

$$\phi_0 = -\frac{k^2 m\Delta}{l}, \phi_1 = \frac{6k^2 m\vartheta_2\sqrt{\Delta}}{l}, \ \phi_2 = -\frac{6B^2 k^2 m}{l}, H = \frac{\vartheta_3}{2\vartheta_2} + \frac{\sqrt{\Delta}}{\vartheta_2},$$
$$\upsilon = \frac{1}{2}n + \sqrt{1 - mk^2\Delta}, \ \phi_{-1} = 0, \phi_{-2} = 0. \tag{40}$$

By inserting the obtained values of constants from Eq. (40) along with the values from Eqs. (5) into (15), we derive the subsequent solutions for Set 5:

$$w_{51}(\eta) = -\frac{k^2 m\Delta}{l} + \frac{6k^2 m\vartheta_2\sqrt{\Delta}}{l}\left(\frac{\vartheta_3}{2\vartheta_2} + \frac{\sqrt{\Delta}}{\vartheta_2} + \frac{\sqrt{\vartheta_1\vartheta_2}\left(\theta_1 \cos\left(\sqrt{\vartheta_1\vartheta_2}\eta\right) + \theta_2 \sin\left(\sqrt{\vartheta_1\vartheta_2}\eta\right)\right)}{\vartheta_1\left(\theta_2 \cos\left(\sqrt{\vartheta_1\vartheta_2}\eta\right) - \theta_1 \sin\left(\sqrt{\vartheta_1\vartheta_2}\eta\right)\right)}\right) - \frac{6\vartheta_2^2 k^2 m}{l}\left(\frac{\vartheta_3}{2\vartheta_2} + \frac{\sqrt{\Delta}}{\vartheta_2} + \frac{\sqrt{\vartheta_1\vartheta_2}\left(\theta_1 \cos\left(\sqrt{\vartheta_1\vartheta_2}\eta\right) + \theta_2 \sin\left(\sqrt{\vartheta_1\vartheta_2}\eta\right)\right)}{\vartheta_1\left(\theta_2 \cos\left(\sqrt{\vartheta_1\vartheta_2}\eta\right) - \theta_1 \sin\left(\sqrt{\vartheta_1\vartheta_2}\eta\right)\right)}\right)^2, \tag{41}$$

$$w_{52}(\eta) = -\frac{k^2 m\Delta}{l} + \frac{6k^2 m\vartheta_2\sqrt{\Delta}}{l}\left(\frac{\vartheta_3}{2\vartheta_2} + \frac{\sqrt{\Delta}}{\vartheta_2} - \frac{\sqrt{|\vartheta_1\vartheta_2|}\left(\theta_1 \sinh\left(2\sqrt{|\vartheta_1\vartheta_2|}\eta\right) + \theta_1 \cosh\left(2\sqrt{|\vartheta_1\vartheta_2|}\eta\right) + \theta_2\right)}{\vartheta_1\left(\theta_1 \sinh\left(2\sqrt{|\vartheta_1\vartheta_2|}\eta\right) + \theta_1 \cosh\left(2\sqrt{|\vartheta_1\vartheta_2|}\eta\right) - \theta_2\right)}\right) - \frac{6\vartheta_2^2 k^2 m}{l}\left(\frac{\vartheta_3}{2\vartheta_2} + \frac{\sqrt{\Delta}}{\vartheta_2} - \frac{\sqrt{|\vartheta_1\vartheta_2|}\left(\theta_1 \sinh\left(2\sqrt{|\vartheta_1\vartheta_2|}\eta\right) + \theta_1 \cosh\left(2\sqrt{|\vartheta_1\vartheta_2|}\eta\right) + \theta_2\right)}{\vartheta_1\left(\theta_1 \sinh\left(2\sqrt{|\vartheta_1\vartheta_2|}\eta\right) + \theta_1 \cosh\left(2\sqrt{|\vartheta_1\vartheta_2|}\eta\right) - \theta_2\right)}\right)^2, \tag{42}$$

$$w_{53}(\eta) = -\frac{k^2 m\Delta}{l} + \frac{6k^2 m\vartheta_2\sqrt{\Delta}}{l}\left(\frac{\vartheta_3}{2\vartheta_2} + \frac{\sqrt{\Delta}}{\vartheta_2} - \frac{\theta_1}{\vartheta_2(\theta_1\eta + Q)}\right) - \frac{6\vartheta_2^2 k^2 m}{l}\left(\frac{\vartheta_3}{2\vartheta_2} + \frac{\sqrt{\Delta}}{\vartheta_2} - \frac{\theta_1}{\vartheta_2(\theta_1\eta + Q)}\right)^2, \tag{43}$$

$$w_{54}(\eta) = -\frac{k^2 m\Delta}{l} + \frac{6k^2 m\vartheta_2\sqrt{\Delta}}{l}\left(\frac{1}{\vartheta_2} - \frac{\left(\theta_1 \cosh\left(\frac{\sqrt{\Delta}}{2}\eta\right) + \theta_2 \sinh\left(\frac{\sqrt{\Delta}}{2}\eta\right)\right)}{2\vartheta_2\left(\theta_2 \cosh\left(\frac{\sqrt{\Delta}}{2}\eta\right) + \theta_1 \sinh\left(\frac{\sqrt{\Delta}}{2}\eta\right)\right)}\right) - \frac{6\vartheta_2^2 k^2 m}{l}\left(\frac{1}{\vartheta_2} - \frac{\left(\theta_1 \cosh\left(\frac{\sqrt{\Delta}}{2}\eta\right) + \theta_2 \sinh\left(\frac{\sqrt{\Delta}}{2}\eta\right)\right)}{2\vartheta_2\left(\theta_2 \cosh\left(\frac{\sqrt{\Delta}}{2}\eta\right) + \theta_1 \sinh\left(\frac{\sqrt{\Delta}}{2}\eta\right)\right)}\right)^2, \tag{44}$$

$$w_{55}(\eta) = -\frac{k^2 m\Delta}{l} + \frac{6k^2 m\vartheta_2\sqrt{\Delta}}{l}\left(\frac{\sqrt{\Delta}}{\vartheta_2} - \frac{\sqrt{-\Delta}\left(\theta_1 \cos\left(\frac{\sqrt{-\Delta}}{2}\eta\right) - \theta_2 \sin\left(\frac{\sqrt{-\Delta}}{2}\eta\right)\right)}{2\vartheta_2\left(\theta_1 \sin\left(\frac{\sqrt{-\Delta}}{2}\eta\right) + \theta_2 \cos\left(\frac{\sqrt{-\Delta}}{2}\eta\right)\right)}\right) - \frac{6\vartheta_2^2 k^2 m}{l}\left(\frac{\sqrt{\Delta}}{\vartheta_2} - \frac{\sqrt{-\Delta}\left(\theta_1 \cos\left(\frac{\sqrt{-\Delta}}{2}\eta\right) - \theta_2 \sin\left(\frac{\sqrt{-\Delta}}{2}\eta\right)\right)}{2\vartheta_2\left(\theta_1 \sin\left(\frac{\sqrt{-\Delta}}{2}\eta\right) + \theta_2 \cos\left(\frac{\sqrt{-\Delta}}{2}\eta\right)\right)}\right)^2. \tag{45}$$

Set 6:

$$\phi_1 = \frac{6k^2 mB\sqrt{\Delta}}{l},\ \phi_2 = -\frac{6B^2 k^2 m}{l}, \phi_0 = 0, \phi_{-1} = 0, \phi_{-2} = 0, H = \frac{\vartheta_3}{2\vartheta_2} + \frac{\sqrt{\Delta}}{\vartheta_2},$$
$$v = \frac{1}{2}n + \sqrt{1 + mk^2\Delta}. \tag{46}$$

By inserting the obtained values of constants from Eq. (46) along with the values from Eqs. (5) into (15), we derive the subsequent solutions for Set 6:

$$w_{61}(\eta) = \frac{6k^2 m\vartheta_2\sqrt{\Delta}}{l}\left(\frac{\vartheta_3}{2\vartheta_2} + \frac{\sqrt{\Delta}}{\vartheta_2} + \frac{\sqrt{\vartheta_1\vartheta_2}\left(\theta_1 \cos\left(\sqrt{\vartheta_1\vartheta_2}\eta\right) + \theta_2 \sin\left(\sqrt{\vartheta_1\vartheta_2}\eta\right)\right)}{\vartheta_1\left(\theta_2 \cos\left(\sqrt{\vartheta_1\vartheta_2}\eta\right) - \theta_1 \sin\left(\sqrt{\vartheta_1\vartheta_2}\eta\right)\right)}\right) - \frac{6\vartheta_2^2 k^2 m}{l}\left(\frac{\vartheta_3}{2\vartheta_2} + \frac{\sqrt{\Delta}}{\vartheta_2} + \frac{\sqrt{\vartheta_1\vartheta_2}\left(\theta_1 \cos\left(\sqrt{\vartheta_1\vartheta_2}\eta\right) + \theta_2 \sin\left(\sqrt{\vartheta_1\vartheta_2}\eta\right)\right)}{\vartheta_1\left(\theta_2 \cos\left(\sqrt{\vartheta_1\vartheta_2}\eta\right) - \theta_1 \sin\left(\sqrt{\vartheta_1\vartheta_2}\eta\right)\right)}\right)^2, \tag{47}$$

$$w_{62}(\eta) = \frac{6k^2 m\vartheta_2\sqrt{\Delta}}{l}\left(\frac{\vartheta_3}{2\vartheta_2} + \frac{\sqrt{\Delta}}{\vartheta_2} - \frac{\sqrt{|\vartheta_1\vartheta_2|}\left(\theta_1 \sinh\left(2\sqrt{|\vartheta_1\vartheta_2|}\eta\right) + \theta_1 \cosh\left(2\sqrt{|\vartheta_1\vartheta_2|}\eta\right) + \theta_2\right)}{\vartheta_1\left(\theta_1 \sinh\left(2\sqrt{|\vartheta_1\vartheta_2|}\eta\right) + \theta_1 \cosh\left(2\sqrt{|\vartheta_1\vartheta_2|}\eta\right) - \theta_2\right)}\right) - \frac{6\vartheta_2^2 k^2 m}{l}\left(\frac{\vartheta_3}{2\vartheta_2} + \frac{\sqrt{\Delta}}{\vartheta_2} - \frac{\sqrt{|\vartheta_1\vartheta_2|}\left(\theta_1 \sinh\left(2\sqrt{|\vartheta_1\vartheta_2|}\eta\right) + \theta_1 \cosh\left(2\sqrt{|\vartheta_1\vartheta_2|}\eta\right) + \theta_2\right)}{\vartheta_1\left(\theta_1 \sinh\left(2\sqrt{|\vartheta_1\vartheta_2|}\eta\right) + \theta_1 \cosh\left(2\sqrt{|\vartheta_1\vartheta_2|}\eta\right) - \theta_2\right)}\right)^2, \tag{48}$$

$$w_{63}(\eta) = \frac{6k^2 m\vartheta_2\sqrt{\Delta}}{l}\left(\frac{\vartheta_3}{2\vartheta_2} + \frac{\sqrt{\Delta}}{\vartheta_2} - \frac{\theta_1}{\vartheta_2(\theta_1\eta + Q)}\right) - \frac{6\vartheta_2^2 k^2 m}{l}\left(\frac{\vartheta_3}{2\vartheta_2} + \frac{\sqrt{\Delta}}{\vartheta_2} - \frac{\theta_1}{\vartheta_2(\theta_1\eta + Q)}\right)^2, \tag{49}$$

$$w_{64}(\eta) = \frac{6k^2m\vartheta_2\sqrt{\Delta}}{l}\left(\frac{1}{\vartheta_2} - \frac{\left(\theta_1 \cos h\left(\frac{\sqrt{\Delta}}{2}\eta\right) + \theta_2 \sin h\left(\frac{\sqrt{\Delta}}{2}\eta\right)\right)}{2\vartheta_2\left(\theta_2 \cos h\left(\frac{\sqrt{\Delta}}{2}\eta\right) + \theta_1 \sin h\left(\frac{\sqrt{\Delta}}{2}\eta\right)\right)}\right) - \frac{6\vartheta_2^2k^2m}{l}\left(\frac{1}{\vartheta_2} - \frac{\left(\theta_1 \cos h\left(\frac{\sqrt{\Delta}}{2}\eta\right) + \theta_2 \sin h\left(\frac{\sqrt{\Delta}}{2}\eta\right)\right)}{2\vartheta_2\left(\theta_2 \cos h\left(\frac{\sqrt{\Delta}}{2}\eta\right) + \theta_1 \sin h\left(\frac{\sqrt{\Delta}}{2}\eta\right)\right)}\right)^2, \tag{50}$$

$$w_{65}(\eta) = \frac{6k^2m\vartheta_2\sqrt{\Delta}}{l}\left(\frac{\sqrt{\Delta}}{\vartheta_2} - \frac{\sqrt{-\Delta}\left(\theta_1 \cos\left(\frac{\sqrt{-\Delta}}{2}\eta\right) - \theta_2 \sin\left(\frac{\sqrt{-\Delta}}{2}\eta\right)\right)}{2\vartheta_2\left(\theta_1 \sin\left(\frac{\sqrt{-\Delta}}{2}\eta\right) + \theta_2 \cos\left(\frac{\sqrt{-\Delta}}{2}\eta\right)\right)}\right) - \frac{6\vartheta_2^2k^2m}{l}\left(\frac{\sqrt{\Delta}}{\vartheta_2} - \frac{\sqrt{-\Delta}\left(\theta_1 \cos\left(\frac{\sqrt{-\Delta}}{2}\eta\right) - \theta_2 \sin\left(\frac{\sqrt{-\Delta}}{2}\eta\right)\right)}{2\vartheta_2\left(\theta_1 \sin\left(\frac{\sqrt{-\Delta}}{2}\eta\right) + \theta_2 \cos\left(\frac{\sqrt{-\Delta}}{2}\eta\right)\right)}\right)^2. \tag{51}$$

Set 7:

$$\phi_0 = \frac{k^2m\Delta}{2l}, \phi_{-2} = -\frac{3k^2m\Delta^2}{8l\vartheta_2^2}, H = \frac{\vartheta_3}{2\vartheta_2}, \nu = \frac{1}{2}n - \sqrt{1 - mk^2\Delta}, \phi_1 = 0, \phi_2 = 0, \phi_{-1} = 0. \tag{52}$$

By inserting the obtained values of constants from Eq. (52) along with the values from Eqs. (5) into (15), we derive the subsequent solutions for Set 7:

$$w_{71}(\eta) = \frac{k^2m\Delta}{2l} - \frac{3k^2m\Delta^2}{8l\vartheta_2^2}\left(\frac{\vartheta_3}{2\vartheta_2} + \frac{\sqrt{\vartheta_1\vartheta_2}\left(\theta_1 \cos\left(\sqrt{\vartheta_1\vartheta_2}\eta\right) + \theta_2 \sin\left(\sqrt{\vartheta_1\vartheta_2}\eta\right)\right)}{\vartheta_1\left(\theta_2 \cos\left(\sqrt{\vartheta_1\vartheta_2}\eta\right) - \theta_1 \sin\left(\sqrt{\vartheta_1\vartheta_2}\eta\right)\right)}\right)^{-2}, \tag{53}$$

$$w_{72}(\eta) = \frac{k^2m\Delta}{2l} - \frac{3k^2m\Delta^2}{8l\vartheta_2^2}\left(\frac{\vartheta_3}{2\vartheta_2} - \frac{\sqrt{|\vartheta_1\vartheta_2|}\left(\theta_1 \sin h\left(2\sqrt{|\vartheta_1\vartheta_2|}\eta\right) + \theta_1 \cos h\left(2\sqrt{|\vartheta_1\vartheta_2|}\eta\right) + \theta_2\right)}{\vartheta_1\left(\theta_1 \sin h\left(2\sqrt{|\vartheta_1\vartheta_2|}\eta\right) + \theta_1 \cos h\left(2\sqrt{|\vartheta_1\vartheta_2|}\eta\right) - \theta_2\right)}\right)^{-2}, \tag{54}$$

$$w_{73}(\eta) = \frac{k^2m\Delta}{2l} - \frac{3k^2m\Delta^2}{8l\vartheta_2^2}\left(\frac{\vartheta_3}{2\vartheta_2} - \frac{\theta_1}{\vartheta_2\left(\theta_1\eta + Q\right)}\right)^{-2}, \tag{55}$$

$$w_{74}(\eta) = \frac{k^2m\Delta}{2l} + \frac{3k^2m\Delta^2}{8l\vartheta_2^2}\left(\frac{\sqrt{\Delta}\left(\theta_1 \cos h\left(\frac{\sqrt{\Delta}}{2}\eta\right) + \theta_2 \sin h\left(\frac{\sqrt{\Delta}}{2}\eta\right)\right)}{2\vartheta_2\left(\theta_2 \cos h\left(\frac{\sqrt{\Delta}}{2}\eta\right) + \theta_1 \sin h\left(\frac{\sqrt{\Delta}}{2}\eta\right)\right)}\right)^{-2}, \tag{56}$$

$$w_{75}(\eta) = \frac{k^2m\Delta}{2l} + \frac{3k^2m\Delta^2}{8l\vartheta_2^2}\left(\frac{\sqrt{-\Delta}\left(\theta_1 \cos\left(\frac{\sqrt{-\Delta}}{2}\eta\right) - \theta_2 \sin\left(\frac{\sqrt{-\Delta}}{2}\eta\right)\right)}{2\vartheta_2\left(\theta_1 \sin\left(\frac{\sqrt{-\Delta}}{2}\eta\right) + \theta_2 \cos\left(\frac{\sqrt{-\Delta}}{2}\eta\right)\right)}\right)^{-2}. \tag{57}$$

Set 8:

$$\phi_{-1} = -\frac{mk^2\Delta^2}{l\vartheta_2\sqrt{3\Delta}}, \phi_{-2} = -\frac{mk^2\Delta^2}{6l\vartheta_2^2}, H = \frac{\vartheta_3}{2\vartheta_2} + \frac{\sqrt{3\Delta}}{6\vartheta_2}, \nu = \frac{1}{2}n + \sqrt{1 - mk^2\Delta}\,, \phi_0 = \phi_1 = \phi_2 = 0. \tag{58}$$

By inserting the obtained values of constants from Eq. (58) along with the values from Eqs. (5) into (15), we derive the subsequent solutions for Set 8:

$$w_{81}(\eta) = -\frac{mk^2\Delta^2}{l\vartheta_2\sqrt{3\Delta}}\left(\frac{\vartheta_3}{2\vartheta_2}+\frac{\sqrt{3\Delta}}{6\vartheta_2}+\frac{\sqrt{\vartheta_1\vartheta_2}\left(\theta_1\cos\left(\sqrt{\vartheta_1\vartheta_2}\eta\right)+\theta_2\sin\left(\sqrt{\vartheta_1\vartheta_2}\eta\right)\right)}{\vartheta_1\left(\theta_2\cos\left(\sqrt{\vartheta_1\vartheta_2}\eta\right)-\theta_1\sin\left(\sqrt{\vartheta_1\vartheta_2}\eta\right)\right)}\right)^{-1}$$
$$-\frac{mk^2\Delta^2}{6l\vartheta_2^2}\left(\frac{\vartheta_3}{2\vartheta_2}+\frac{\sqrt{3\Delta}}{6\vartheta_2}+\frac{\sqrt{\vartheta_1\vartheta_2}\left(\theta_1\cos\left(\sqrt{\vartheta_1\vartheta_2}\eta\right)+\theta_2\sin\left(\sqrt{\vartheta_1\vartheta_2}\eta\right)\right)}{\vartheta_1\left(\theta_2\cos\left(\sqrt{\vartheta_1\vartheta_2}\eta\right)-\theta_1\sin\left(\sqrt{\vartheta_1\vartheta_2}\eta\right)\right)}\right)^{-2}, \tag{59}$$

$$w_{82}(\eta) = -\frac{mk^2\Delta^2}{l\vartheta_2\sqrt{3\Delta}}\left(\frac{\vartheta_3}{2\vartheta_2}+\frac{\sqrt{3\Delta}}{6\vartheta_2}-\frac{\sqrt{|\vartheta_1\vartheta_2|}\left(\theta_1\sinh\left(2\sqrt{|\vartheta_1\vartheta_2|}\eta\right)+\theta_1\cosh\left(2\sqrt{|\vartheta_1\vartheta_2|}\eta\right)+\theta_2\right)}{\vartheta_1\left(\theta_1\sinh\left(2\sqrt{|\vartheta_1\vartheta_2|}\eta\right)+\theta_1\cosh\left(2\sqrt{|\vartheta_1\vartheta_2|}\eta\right)-\theta_2\right)}\right)^{-1}$$
$$-\frac{mk^2\Delta^2}{6l\vartheta_2^2}\left(\frac{\vartheta_3}{2\vartheta_2}+\frac{\sqrt{3\Delta}}{6\vartheta_2}-\frac{\sqrt{|\vartheta_1\vartheta_2|}\left(\theta_1\sinh\left(2\sqrt{|\vartheta_1\vartheta_2|}\eta\right)+\theta_1\cosh\left(2\sqrt{|\vartheta_1\vartheta_2|}\eta\right)+\theta_2\right)}{\vartheta_1\left(\theta_1\sinh\left(2\sqrt{|\vartheta_1\vartheta_2|}\eta\right)+\theta_1\cosh\left(2\sqrt{|\vartheta_1\vartheta_2|}\eta\right)-\theta_2\right)}\right)^{-2}, \tag{60}$$

$$w_{83}(\eta) = -\frac{mk^2\Delta^2}{l\vartheta_2\sqrt{3\Delta}}\left(\frac{\vartheta_3}{2\vartheta_2}+\frac{\sqrt{3\Delta}}{6\vartheta_2}-\frac{\theta_1}{\vartheta_2\left(\theta_1\eta+Q\right)}\right)^{-1}-\frac{mk^2\Delta^2}{6l\vartheta_2^2}\left(\frac{\vartheta_3}{2\vartheta_2}+\frac{\sqrt{3\Delta}}{6\vartheta_2}-\frac{\theta_1}{\vartheta_2\left(\theta_1\eta+Q\right)}\right)^{-2}, \tag{61}$$

$$w_{84}(\eta) = -\frac{mk^2\Delta^2}{l\vartheta_2\sqrt{3\Delta}}\left(\frac{\sqrt{3\Delta}}{6\vartheta_2}-\frac{\sqrt{\Delta}\left(\theta_1\cosh\left(\frac{\sqrt{\Delta}}{2}\eta\right)+\theta_2\sinh\left(\frac{\sqrt{\Delta}}{2}\eta\right)\right)}{2\vartheta_2\left(\theta_2\cosh\left(\frac{\sqrt{\Delta}}{2}\eta\right)+\theta_1\sinh\left(\frac{\sqrt{\Delta}}{2}\eta\right)\right)}\right)^{-1}$$
$$-\frac{mk^2\Delta^2}{6l\vartheta_2^2}\left(\frac{\sqrt{3\Delta}}{6\vartheta_2}-\frac{\sqrt{\Delta}\left(\theta_1\cosh\left(\frac{\sqrt{\Delta}}{2}\eta\right)+\theta_2\sinh\left(\frac{\sqrt{\Delta}}{2}\eta\right)\right)}{2\vartheta_2\left(\theta_2\cosh\left(\frac{\sqrt{\Delta}}{2}\eta\right)+\theta_1\sinh\left(\frac{\sqrt{\Delta}}{2}\eta\right)\right)}\right)^{-2}, \tag{62}$$

$$w_{85}(\eta) = -\frac{mk^2\Delta^2}{l\vartheta_2\sqrt{3\Delta}}\left(\frac{\sqrt{3\Delta}}{6\vartheta_2}-\frac{\sqrt{-\Delta}\left(\theta_1\cos\left(\frac{\sqrt{-\Delta}}{2}\eta\right)-\theta_2\sin\left(\frac{\sqrt{-\Delta}}{2}\eta\right)\right)}{2\vartheta_2\left(\theta_1\sin\left(\frac{\sqrt{-\Delta}}{2}\eta\right)+\theta_2\cos\left(\frac{\sqrt{-\Delta}}{2}\eta\right)\right)}\right)^{-1}$$
$$-\frac{mk^2\Delta^2}{6l\vartheta_2^2}\left(\frac{\sqrt{3\Delta}}{6\vartheta_2}-\frac{\sqrt{-\Delta}\left(\theta_1\cos\left(\frac{\sqrt{-\Delta}}{2}\eta\right)-\theta_2\sin\left(\frac{\sqrt{-\Delta}}{2}\eta\right)\right)}{2\vartheta_2\left(\theta_1\sin\left(\frac{\sqrt{-\Delta}}{2}\eta\right)+\theta_2\cos\left(\frac{\sqrt{-\Delta}}{2}\eta\right)\right)}\right)^{-2}. \tag{63}$$

Set 9:

$$\phi_0=\frac{mk^2\Delta}{l},\ \phi_{-1}=-\frac{mk^2\Delta^2}{l\vartheta_2\sqrt{3\Delta}},\ \phi_{-2}=-\frac{mk^2\Delta^2}{6l\vartheta_2^2},\ H=\frac{\vartheta_3}{2\vartheta_2}+\frac{\sqrt{3\Delta}}{6\vartheta_2},$$
$$\nu=\frac{1}{2}n+\sqrt{1-mk^2\Delta},\phi_1=\phi_2=0. \tag{64}$$

By inserting the obtained values of constants from Eq. (64) along with the values from Eqs. (5) into (15), we derive the subsequent solutions for Set 9:

$$w_{91}(\eta) = \frac{mk^2\Delta}{l} - \frac{mk^2\Delta^2}{l\vartheta_2\sqrt{3\Delta}}\left(\frac{\vartheta_3}{2\vartheta_2} + \frac{\sqrt{3\Delta}}{6\vartheta_2} + \frac{\sqrt{\vartheta_1\vartheta_2}\left(\theta_1\cos\left(\sqrt{\vartheta_1\vartheta_2}\eta\right) + \theta_2\sin\left(\sqrt{\vartheta_1\vartheta_2}\eta\right)\right)}{\vartheta_1\left(\theta_2\cos\left(\sqrt{\vartheta_1\vartheta_2}\eta\right) - \theta_1\sin\left(\sqrt{\vartheta_1\vartheta_2}\eta\right)\right)}\right)^{-1}$$
$$- \frac{mk^2\Delta^2}{6l\vartheta_2^2}\left(\frac{\vartheta_3}{2\vartheta_2} + \frac{\sqrt{3\Delta}}{6\vartheta_2} + \frac{\sqrt{\vartheta_1\vartheta_2}\left(\theta_1\cos\left(\sqrt{\vartheta_1\vartheta_2}\eta\right) + \theta_2\sin\left(\sqrt{\vartheta_1\vartheta_2}\eta\right)\right)}{\vartheta_1\left(\theta_2\cos\left(\sqrt{\vartheta_1\vartheta_2}\eta\right) - \theta_1\sin\left(\sqrt{\vartheta_1\vartheta_2}\eta\right)\right)}\right)^{-2}, \tag{65}$$

$$w_{92}(\eta) = \frac{mk^2\Delta}{l} - \frac{mk^2\Delta^2}{l\vartheta_2\sqrt{3\Delta}}\left(\frac{\vartheta_3}{2\vartheta_2} + \frac{\sqrt{3\Delta}}{6\vartheta_2} - \frac{\sqrt{|\vartheta_1\vartheta_2|}\left(\theta_1\sinh\left(2\sqrt{|\vartheta_1\vartheta_2|}\eta\right) + \theta_1\cosh\left(2\sqrt{|\vartheta_1\vartheta_2|}\eta\right) + \theta_2\right)}{\vartheta_1\left(\theta_1\sinh\left(2\sqrt{|\vartheta_1\vartheta_2|}\eta\right) + \theta_1\cosh\left(2\sqrt{|\vartheta_1\vartheta_2|}\eta\right) - \theta_2\right)}\right)^{-1}$$
$$- \frac{mk^2\Delta^2}{6l\vartheta_2^2}\left(\frac{\vartheta_3}{2\vartheta_2} + \frac{\sqrt{3\Delta}}{6\vartheta_2} - \frac{\sqrt{|\vartheta_1\vartheta_2|}\left(\theta_1\sinh\left(2\sqrt{|\vartheta_1\vartheta_2|}\eta\right) + \theta_1\cosh\left(2\sqrt{|\vartheta_1\vartheta_2|}\eta\right) + \theta_2\right)}{\vartheta_1\left(\theta_1\sinh\left(2\sqrt{|\vartheta_1\vartheta_2|}\eta\right) + \theta_1\cosh\left(2\sqrt{|\vartheta_1\vartheta_2|}\eta\right) - \theta_2\right)}\right)^{-2}, \tag{66}$$

$$w_{93}(\eta) = \frac{mk^2\Delta}{l} - \frac{mk^2\Delta^2}{l\vartheta_2\sqrt{3\Delta}}\left(\frac{\vartheta_3}{2\vartheta_2} + \frac{\sqrt{3\Delta}}{6\vartheta_2} - \frac{\theta_1}{\vartheta_2\left(\theta_1\eta + Q\right)}\right)^{-1}$$
$$- \frac{mk^2\Delta^2}{6l\vartheta_2^2}\left(\frac{\vartheta_3}{2\vartheta_2} + \frac{\sqrt{3\Delta}}{6\vartheta_2} - \frac{\theta_1}{\vartheta_2\left(\theta_1\eta + Q\right)}\right)^{-2}, \tag{67}$$

$$w_{94}(\eta) = \frac{mk^2\Delta}{l} - \frac{mk^2\Delta^2}{l\vartheta_2\sqrt{3\Delta}}\left(\frac{\sqrt{3\Delta}}{6\vartheta_2} - \frac{\sqrt{\Delta}\left(\theta_1\cosh\left(\frac{\sqrt{\Delta}}{2}\eta\right) + \theta_2\sinh\left(\frac{\sqrt{\Delta}}{2}\eta\right)\right)}{2\vartheta_2\left(\theta_2\cosh\left(\frac{\sqrt{\Delta}}{2}\eta\right) + \theta_1\sinh\left(\frac{\sqrt{\Delta}}{2}\eta\right)\right)}\right)^{-1}$$
$$- \frac{mk^2\Delta^2}{6l\vartheta_2^2}\left(\frac{\sqrt{3\Delta}}{6\vartheta_2} - \frac{\sqrt{\Delta}\left(\theta_1\cosh\left(\frac{\sqrt{\Delta}}{2}\eta\right) + \theta_2\sinh\left(\frac{\sqrt{\Delta}}{2}\eta\right)\right)}{2\vartheta_2\left(\theta_2\cosh\left(\frac{\sqrt{\Delta}}{2}\eta\right) + \theta_1\sinh\left(\frac{\sqrt{\Delta}}{2}\eta\right)\right)}\right)^{-2}, \tag{68}$$

$$w_{95}(\eta) = \frac{mk^2\Delta}{l} - \frac{mk^2\Delta^2}{l\vartheta_2\sqrt{3\Delta}}\left(\frac{\sqrt{3\Delta}}{6\vartheta_2} - \frac{\sqrt{-\Delta}\left(\theta_1\cos\left(\frac{\sqrt{-\Delta}}{2}\eta\right) - \theta_2\sin\left(\frac{\sqrt{-\Delta}}{2}\eta\right)\right)}{2\vartheta_2\left(\theta_1\sin\left(\frac{\sqrt{-\Delta}}{2}\eta\right) + \theta_2\cos\left(\frac{\sqrt{-\Delta}}{2}\eta\right)\right)}\right)^{-1}$$
$$- \frac{mk^2\Delta^2}{6l\vartheta_2^2}\left(\frac{\sqrt{3\Delta}}{6\vartheta_2} - \frac{\sqrt{-\Delta}\left(\theta_1\cos\left(\frac{\sqrt{-\Delta}}{2}\eta\right) - \theta_2\sin\left(\frac{\sqrt{-\Delta}}{2}\eta\right)\right)}{2\vartheta_2\left(\theta_1\sin\left(\frac{\sqrt{-\Delta}}{2}\eta\right) + \theta_2\cos\left(\frac{\sqrt{-\Delta}}{2}\eta\right)\right)}\right)^{-2}. \tag{69}$$

Set 10:

$$H = H,\ \nu = \frac{1}{2}n + \sqrt{1 - mk^2\Delta},\ \phi_0 = -\frac{mk^2\left(6\vartheta_2^2H^2 - 6\vartheta_2\vartheta_3H + 2\vartheta_1\vartheta_2 + \vartheta_3^2\right)}{l},$$
$$\phi_1 = 0, \phi_2 = 0, \phi_{-1} = \frac{6mk^2\left(\vartheta_2H^2 - \vartheta_3H + \vartheta_1\right)\left(2\vartheta_2H - \vartheta_3\right)}{l},$$
$$\phi_{-2} = -\frac{6mk^2\left(\vartheta_2^2H^4 - 2\vartheta_2\vartheta_3H^3 + 2\vartheta_1\vartheta_2H^2 + \vartheta_3^2H^2 - 2\vartheta_1\vartheta_3H + \vartheta_1^2\right)}{l}. \tag{70}$$

By inserting the obtained values of constants from Eq. (70) along with the values from Eqs. (5) into (15), we derive the subsequent solutions for Set 10:

$$w_{101}(\eta) = -\frac{mk^2\left(6\vartheta_2^2H^2 - 6\vartheta_2\vartheta_3H + 2\vartheta_1\vartheta_2 + \vartheta_3^2\right)}{l} - \frac{6mk^2\left(\vartheta_2H^2 - \vartheta_3H + \vartheta_1\right)\left(2\vartheta_2H - \vartheta_3\right)}{l}$$
$$\times\left(H + \frac{\sqrt{\vartheta_1\vartheta_2}\left(\theta_1\cos\left(\sqrt{\vartheta_1\vartheta_2}\eta\right) + \theta_2\sin\left(\sqrt{\vartheta_1\vartheta_2}\eta\right)\right)}{\vartheta_1\left(\theta_2\cos\left(\sqrt{\vartheta_1\vartheta_2}\eta\right) - \theta_1\sin\left(\sqrt{\vartheta_1\vartheta_2}\eta\right)\right)}\right)^{-1}$$
$$-\frac{6mk^2\left(\vartheta_2^2H^4 - 2\vartheta_2\vartheta_3H^3 + 2\vartheta_1\vartheta_2H^2 + \vartheta_3^2H^2 - 2\vartheta_1\vartheta_3H + \vartheta_1^2\right)}{l}$$
$$\times\left(H + \frac{\sqrt{\vartheta_1\vartheta_2}\left(\theta_1\cos\left(\sqrt{\vartheta_1\vartheta_2}\eta\right) + \theta_2\sin\left(\sqrt{\vartheta_1\vartheta_2}\eta\right)\right)}{\vartheta_1\left(\theta_2\cos\left(\sqrt{\vartheta_1\vartheta_2}\eta\right) - \theta_1\sin\left(\sqrt{\vartheta_1\vartheta_2}\eta\right)\right)}\right)^{-2}, \tag{71}$$

$$w_{102}(\eta) = -\frac{mk^2\left(6\vartheta_2^2H^2 - 6\vartheta_2\vartheta_3H + 2\vartheta_1\vartheta_2 + \vartheta_3^2\right)}{l}$$
$$-\frac{6mk^2\left(\vartheta_2H^2 - \vartheta_3H + \vartheta_1\right)\left(2\vartheta_2H - \vartheta_3\right)}{l}\left(H - \frac{\sqrt{|\vartheta_1\vartheta_2|}\left(\theta_1\sinh\left(2\sqrt{|\vartheta_1\vartheta_2|}\eta\right) + \theta_1\cosh\left(2\sqrt{|\vartheta_1\vartheta_2|}\eta\right) + \theta_2\right)}{\vartheta_1\left(\theta_1\sinh\left(2\sqrt{|\vartheta_1\vartheta_2|}\eta\right) + \theta_1\cosh\left(2\sqrt{|\vartheta_1\vartheta_2|}\eta\right) - \theta_2\right)}\right)^{-1}$$
$$-\frac{6mk^2\left(\vartheta_2^2H^4 - 2\vartheta_2\vartheta_3H^3 + 2\vartheta_1\vartheta_2H^2 + \vartheta_3^2H^2 - 2\vartheta_1\vartheta_3H + \vartheta_1^2\right)}{l}$$
$$\times\left(H - \frac{\sqrt{|\vartheta_1\vartheta_2|}\left(\theta_1\sinh\left(2\sqrt{|\vartheta_1\vartheta_2|}\eta\right) + \theta_1\cosh\left(2\sqrt{|\vartheta_1\vartheta_2|}\eta\right) + \theta_2\right)}{\vartheta_1\left(\theta_1\sinh\left(2\sqrt{|\vartheta_1\vartheta_2|}\eta\right) + \theta_1\cosh\left(2\sqrt{|\vartheta_1\vartheta_2|}\eta\right) - \theta_2\right)}\right)^{-2}, \tag{72}$$

$$w_{103}(\eta) = -\frac{mk^2\left(6\vartheta_2^2H^2 - 6\vartheta_2\vartheta_3H + 2\vartheta_1\vartheta_2 + \vartheta_3^2\right)}{l}$$
$$-\frac{6mk^2\left(\vartheta_2H^2 - \vartheta_3H + \vartheta_1\right)\left(2\vartheta_2H - \vartheta_3\right)}{l}\left(H - \frac{\theta_1}{\vartheta_2\left(\theta_1\eta + Q\right)}\right)^{-1}$$
$$-\frac{6mk^2\left(\vartheta_2^2H^4 - 2\vartheta_2\vartheta_3H^3 + 2\vartheta_1\vartheta_2H^2 + \vartheta_3^2H^2 - 2\vartheta_1\vartheta_3H + \vartheta_1^2\right)}{l}\left(H - \frac{\theta_1}{\vartheta_2\left(\theta_1\eta + Q\right)}\right)^{-2}, \tag{73}$$

$$w_{104}(\eta) = -\frac{mk^2\left(6\vartheta_2^2H^2 - 6\vartheta_2\vartheta_3H + 2\vartheta_1\vartheta_2 + \vartheta_3^2\right)}{l}$$
$$-\frac{6mk^2\left(\vartheta_2H^2 - \vartheta_3H + \vartheta_1\right)\left(2\vartheta_2H - \vartheta_3\right)}{l}\left(H - \frac{\vartheta_3}{2\vartheta_2} - \frac{\sqrt{\Delta}\left(\theta_1\cosh\left(\frac{\sqrt{\Delta}}{2}\eta\right) + \theta_2\sinh\left(\frac{\sqrt{\Delta}}{2}\eta\right)\right)}{2\vartheta_2\left(\theta_2\cosh\left(\frac{\sqrt{\Delta}}{2}\eta\right) + \theta_1\sinh\left(\frac{\sqrt{\Delta}}{2}\eta\right)\right)}\right)^{-1}$$
$$-\frac{6mk^2\left(\vartheta_2^2H^4 - 2\vartheta_2\vartheta_3H^3 + 2\vartheta_1\vartheta_2H^2 + \vartheta_3^2H^2 - 2\vartheta_1\vartheta_3H + \vartheta_1^2\right)}{l}$$
$$\times\left(H - \frac{\vartheta_3}{2\vartheta_2} - \frac{\sqrt{\Delta}\left(\theta_1\cosh\left(\frac{\sqrt{\Delta}}{2}\eta\right) + \theta_2\sinh\left(\frac{\sqrt{\Delta}}{2}\eta\right)\right)}{2\vartheta_2\left(\theta_2\cosh\left(\frac{\sqrt{\Delta}}{2}\eta\right) + \theta_1\sinh\left(\frac{\sqrt{\Delta}}{2}\eta\right)\right)}\right)^{-2}, \tag{74}$$

$$w_{105}(\eta) = -\frac{mk^2\left(6\vartheta_2^2H^2 - 6\vartheta_2\vartheta_3H + 2\vartheta_1\vartheta_2 + \vartheta_3^2\right)}{l}$$
$$-\frac{6mk^2\left(\vartheta_2H^2 - \vartheta_3H + \vartheta_1\right)\left(2\vartheta_2H - \vartheta_3\right)}{l}\left(H - \frac{\vartheta_3}{2\vartheta_2} - \frac{\sqrt{-\Delta}\left(\theta_1\cos\left(\frac{\sqrt{-\Delta}}{2}\eta\right) - \theta_2\sin\left(\frac{\sqrt{-\Delta}}{2}\eta\right)\right)}{2\vartheta_2\left(\theta_1\sin\left(\frac{\sqrt{-\Delta}}{2}\eta\right) + \theta_2\cos\left(\frac{\sqrt{-\Delta}}{2}\eta\right)\right)}\right)^{-1}$$
$$-\frac{6mk^2\left(\vartheta_2^2H^4 - 2\vartheta_2\vartheta_3H^3 + 2\vartheta_1\vartheta_2H^2 + \vartheta_3^2H^2 - 2\vartheta_1\vartheta_3H + \vartheta_1^2\right)}{l}$$
$$\times\left(H - \frac{\vartheta_3}{2\vartheta_2} - \frac{\sqrt{-\Delta}\left(\theta_1\cos\left(\frac{\sqrt{-\Delta}}{2}\eta\right) - \theta_2\sin\left(\frac{\sqrt{-\Delta}}{2}\eta\right)\right)}{2\vartheta_2\left(\theta_1\sin\left(\frac{\sqrt{-\Delta}}{2}\eta\right) + \theta_2\cos\left(\frac{\sqrt{-\Delta}}{2}\eta\right)\right)}\right)^{-2}. \tag{75}$$

Set 11:

$$H = H,\ \nu = \frac{1}{2}n + \sqrt{1 + mk^2\Delta},\ \phi_0 = -\frac{6mk^2\vartheta_2\left(\vartheta_2^2H^2 - \vartheta_3H + \vartheta_1\right)}{l},\ \phi_1 = 0, \phi_2 = 0,$$
$$\phi_{-1} = \frac{6mk^2\left(\vartheta_2H^2 - \vartheta_3H + \vartheta_1\right)\left(2\vartheta_2H - \vartheta_3\right)}{l},\ \phi_{-2} = -\frac{6mk^2\left(\vartheta_2H^2 - \vartheta_3H + \vartheta_1\right)^2}{l}. \tag{76}$$

By inserting the obtained values of constants from Eq. (76) along with the values from Eqs. (5) into (15), we derive the subsequent solutions for Set 11:

$$w_{111}(\eta) = -\frac{6mk^2\vartheta_2\left(\vartheta_2^2H^2 - \vartheta_3H + \vartheta_1\right)}{l}$$
$$+\frac{6mk^2\left(\vartheta_2H^2 - \vartheta_3H + \vartheta_1\right)\left(2\vartheta_2H - \vartheta_3\right)}{l}\left(H + \frac{\sqrt{\vartheta_1\vartheta_2}\left(\theta_1\cos\left(\sqrt{\vartheta_1\vartheta_2}\eta\right) + \theta_2\sin\left(\sqrt{\vartheta_1\vartheta_2}\eta\right)\right)}{\vartheta_1\left(\theta_2\cos\left(\sqrt{\vartheta_1\vartheta_2}\eta\right) - \theta_1\sin\left(\sqrt{\vartheta_1\vartheta_2}\eta\right)\right)}\right)^{-1}$$
$$-\frac{6mk^2\left(\vartheta_2H^2 - \vartheta_3H + \vartheta_1\right)^2}{l}\left(H + \frac{\sqrt{\vartheta_1\vartheta_2}\left(\theta_1\cos\left(\sqrt{\vartheta_1\vartheta_2}\eta\right) + \theta_2\sin\left(\sqrt{\vartheta_1\vartheta_2}\eta\right)\right)}{\vartheta_1\left(\theta_2\cos\left(\sqrt{\vartheta_1\vartheta_2}\eta\right) - \theta_1\sin\left(\sqrt{\vartheta_1\vartheta_2}\eta\right)\right)}\right)^{-2}, \tag{77}$$

$$w_{112}(\eta) = -\frac{6mk^2\vartheta_2\left(\vartheta_2^2H^2 - \vartheta_3H + \vartheta_1\right)}{l} + \frac{6mk^2\left(\vartheta_2H^2 - \vartheta_3H + \vartheta_1\right)\left(2\vartheta_2H - \vartheta_3\right)}{l}$$
$$\times\left(H - \frac{\sqrt{|\vartheta_1\vartheta_2|}\left(\theta_1\sinh\left(2\sqrt{|\vartheta_1\vartheta_2|}\eta\right) + \theta_1\cosh\left(2\sqrt{|\vartheta_1\vartheta_2|}\eta\right) + \theta_2\right)}{\vartheta_1\left(\theta_1\sinh\left(2\sqrt{|\vartheta_1\vartheta_2|}\eta\right) + \theta_1\cosh\left(2\sqrt{|\vartheta_1\vartheta_2|}\eta\right) - \theta_2\right)}\right)^{-1}$$
$$-\frac{6mk^2\left(\vartheta_2H^2 - \vartheta_3H + \vartheta_1\right)^2}{l}\left(H - \frac{\sqrt{|\vartheta_1\vartheta_2|}\left(\theta_1\sinh\left(2\sqrt{|\vartheta_1\vartheta_2|}\eta\right) + \theta_1\cosh\left(2\sqrt{|\vartheta_1\vartheta_2|}\eta\right) + \theta_2\right)}{\vartheta_1\left(\theta_1\sinh\left(2\sqrt{|\vartheta_1\vartheta_2|}\eta\right) + \theta_1\cosh\left(2\sqrt{|\vartheta_1\vartheta_2|}\eta\right) - \theta_2\right)}\right)^{-2}, \tag{78}$$

$$w_{113}(\eta) = -\frac{6mk^2\vartheta_2\left(\vartheta_2^2H^2 - \vartheta_3H + \vartheta_1\right)}{l} + \frac{6mk^2\left(\vartheta_2H^2 - \vartheta_3H + \vartheta_1\right)\left(2\vartheta_2H - \vartheta_3\right)}{l}$$
$$\times\left(H - \frac{\theta_1}{\vartheta_2\left(\theta_1\eta + Q\right)}\right)^{-1} - \frac{6mk^2\left(\vartheta_2H^2 - \vartheta_3H + \vartheta_1\right)^2}{l}\left(H - \frac{\theta_1}{\vartheta_2\left(\theta_1\eta + Q\right)}\right)^{-2}, \tag{79}$$

$$w_{114}(\eta) = -\frac{6mk^2\vartheta_2\left(\vartheta_2^2H^2-\vartheta_3H+\vartheta_1\right)}{l} + \frac{6mk^2\left(\vartheta_2H^2-\vartheta_3H+\vartheta_1\right)(2\vartheta_2H-\vartheta_3)}{l}\left(H-\frac{\vartheta_3}{2\vartheta_2}-\frac{\sqrt{\Delta}\left(\theta_1\cosh\left(\frac{\sqrt{\Delta}}{2}\eta\right)+\theta_2\sinh\left(\frac{\sqrt{\Delta}}{2}\eta\right)\right)}{2\vartheta_2\left(\theta_2\cosh\left(\frac{\sqrt{\Delta}}{2}\eta\right)+\theta_1\sinh\left(\frac{\sqrt{\Delta}}{2}\eta\right)\right)}\right)^{-1} - \frac{6mk^2\left(\vartheta_2H^2-\vartheta_3H+\vartheta_1\right)^2}{l}\left(H-\frac{\vartheta_3}{2\vartheta_2}-\frac{\sqrt{\Delta}\left(\theta_1\cosh\left(\frac{\sqrt{\Delta}}{2}\eta\right)+\theta_2\sinh\left(\frac{\sqrt{\Delta}}{2}\eta\right)\right)}{2\vartheta_2\left(\theta_2\cosh\left(\frac{\sqrt{\Delta}}{2}\eta\right)+\theta_1\sinh\left(\frac{\sqrt{\Delta}}{2}\eta\right)\right)}\right)^{-2}, \tag{80}$$

$$w_{115}(\eta) = -\frac{6mk^2\vartheta_2\left(\vartheta_2^2H^2-\vartheta_3H+\vartheta_1\right)}{l} + \frac{6mk^2\left(\vartheta_2H^2-\vartheta_3H+\vartheta_1\right)(2\vartheta_2H-\vartheta_3)}{l} \times\left(H-\frac{\vartheta_3}{2\vartheta_2}-\frac{\sqrt{-\Delta}\left(\theta_1\cos\left(\frac{\sqrt{-\Delta}}{2}\eta\right)-\theta_2\sin\left(\frac{\sqrt{-\Delta}}{2}\eta\right)\right)}{2\vartheta_2\left(\theta_1\sin\left(\frac{\sqrt{-\Delta}}{2}\eta\right)+\theta_2\cos\left(\frac{\sqrt{-\Delta}}{2}\eta\right)\right)}\right)^{-1} - \frac{6mk^2\left(\vartheta_2H^2-\vartheta_3H+\vartheta_1\right)^2}{l}\left(H-\frac{\vartheta_3}{2\vartheta_2}-\frac{\sqrt{-\Delta}\left(\theta_1\cos\left(\frac{\sqrt{-\Delta}}{2}\eta\right)-\theta_2\sin\left(\frac{\sqrt{-\Delta}}{2}\eta\right)\right)}{2\vartheta_2\left(\theta_1\sin\left(\frac{\sqrt{-\Delta}}{2}\eta\right)+\theta_2\cos\left(\frac{\sqrt{-\Delta}}{2}\eta\right)\right)}\right)^{-2}. \tag{81}$$

Set 12:

$$H=\frac{\vartheta_3}{2\vartheta_2}+\frac{\sqrt{-\Delta}}{2\vartheta_2},\ v=\frac{1}{2}n+\sqrt{1-\Delta mk^2},\ \phi_0=\frac{2mk^2\Delta}{l},\ \phi_1=0,\phi_2=0,$$
$$\phi_{-1}=\frac{3mk^2(-\Delta)^{\frac{3}{2}}}{l\vartheta_2},\ \phi_{-2}=-\frac{3mk^2\Delta^2}{2l\vartheta_2^2}. \tag{82}$$

By inserting the obtained values of constants from Eq. (82) along with the values from Eqs. (5) into (15), we derive the subsequent solutions for Set 12:

$$w_{121}(\eta) = \frac{3mk^2(-\Delta)^{\frac{3}{2}}}{l\vartheta_2}\left(\frac{\vartheta_3}{2\vartheta_2}+\frac{\sqrt{-\Delta}}{2\vartheta_2}+\frac{\sqrt{\vartheta_1\vartheta_2}\left(\theta_1\cos\left(\sqrt{\vartheta_1\vartheta_2}\eta\right)+\theta_2\sin\left(\sqrt{\vartheta_1\vartheta_2}\eta\right)\right)}{\vartheta_1\left(\theta_2\cos\left(\sqrt{\vartheta_1\vartheta_2}\eta\right)-\theta_1\sin\left(\sqrt{\vartheta_1\vartheta_2}\eta\right)\right)}\right)^{-1} - \frac{3mk^2\Delta^2}{2l\vartheta_2^2}\left(\frac{\vartheta_3}{2\vartheta_2}+\frac{\sqrt{-\Delta}}{2\vartheta_2}+\frac{\sqrt{\vartheta_1\vartheta_2}\left(\theta_1\cos\left(\sqrt{\vartheta_1\vartheta_2}\eta\right)+\theta_2\sin\left(\sqrt{\vartheta_1\vartheta_2}\eta\right)\right)}{\vartheta_1\left(\theta_2\cos\left(\sqrt{\vartheta_1\vartheta_2}\eta\right)-\theta_1\sin\left(\sqrt{\vartheta_1\vartheta_2}\eta\right)\right)}\right)^{-2}+\frac{2mk^2\Delta}{l}, \tag{83}$$

$$w_{122}(\eta) = \frac{3mk^2(-\Delta)^{\frac{3}{2}}}{l\vartheta_2}\left(\frac{\vartheta_3}{2\vartheta_2}+\frac{\sqrt{-\Delta}}{2\vartheta_2}-\frac{\sqrt{|\vartheta_1\vartheta_2|}\left(\theta_1\sinh\left(2\sqrt{|\vartheta_1\vartheta_2|}\eta\right)+\theta_1\cosh\left(2\sqrt{|\vartheta_1\vartheta_2|}\eta\right)+\theta_2\right)}{\vartheta_1\left(\theta_1\sinh\left(2\sqrt{|\vartheta_1\vartheta_2|}\eta\right)+\theta_1\cosh\left(2\sqrt{|\vartheta_1\vartheta_2|}\eta\right)-\theta_2\right)}\right)^{-1} - \frac{3mk^2\Delta^2}{2l\vartheta_2^2}\left(\frac{\vartheta_3}{2\vartheta_2}+\frac{\sqrt{-\Delta}}{2\vartheta_2}-\frac{\sqrt{|\vartheta_1\vartheta_2|}\left(\theta_1\sinh\left(2\sqrt{|\vartheta_1\vartheta_2|}\eta\right)+\theta_1\cosh\left(2\sqrt{|\vartheta_1\vartheta_2|}\eta\right)+\theta_2\right)}{\vartheta_1\left(\theta_1\sinh\left(2\sqrt{|\vartheta_1\vartheta_2|}\eta\right)+\theta_1\cosh\left(2\sqrt{|\vartheta_1\vartheta_2|}\eta\right)-\theta_2\right)}\right)^{-2} + \frac{2mk^2\Delta}{l}, \tag{84}$$

$$w_{123}(\eta) = \frac{2mk^2\Delta}{l} + \frac{3mk^2(-\Delta)^{\frac{3}{2}}}{l\vartheta_2}\left(\frac{\vartheta_3}{2\vartheta_2} + \frac{\sqrt{-\Delta}}{2\vartheta_2} - \frac{\theta_1}{\vartheta_2(\theta_1\eta + Q)}\right)^{-1} - \frac{3mk^2\Delta^2}{2l\vartheta_2^2}\left(\frac{\vartheta_3}{2\vartheta_2} + \frac{\sqrt{-\Delta}}{2\vartheta_2} - \frac{\theta_1}{\vartheta_2(\theta_1\eta + Q)}\right)^{-2}, \tag{85}$$

$$w_{124}(\eta) = \frac{3mk^2(-\Delta)^{\frac{3}{2}}}{l\vartheta_2}\left(\frac{\sqrt{-\Delta}}{2\vartheta_2} - \frac{\sqrt{\Delta}\left(\theta_1 \cosh\left(\frac{\sqrt{\Delta}}{2}\eta\right) + \theta_2 \sinh\left(\frac{\sqrt{\Delta}}{2}\eta\right)\right)}{2\vartheta_2\left(\theta_2 \cosh\left(\frac{\sqrt{\Delta}}{2}\eta\right) + \theta_1 \sinh\left(\frac{\sqrt{\Delta}}{2}\eta\right)\right)}\right)^{-1} - \frac{3mk^2\Delta^2}{2l\vartheta_2^2}\left(\frac{\sqrt{-\Delta}}{2\vartheta_2} - \frac{\sqrt{\Delta}\left(\theta_1 \cosh\left(\frac{\sqrt{\Delta}}{2}\eta\right) + \theta_2 \sinh\left(\frac{\sqrt{\Delta}}{2}\eta\right)\right)}{2\vartheta_2\left(\theta_2 \cosh\left(\frac{\sqrt{\Delta}}{2}\eta\right) + \theta_1 \sinh\left(\frac{\sqrt{\Delta}}{2}\eta\right)\right)}\right)^{-2} + \frac{2mk^2\Delta}{l}, \tag{86}$$

$$w_{125}(\eta) = \frac{3mk^2(-\Delta)^{\frac{3}{2}}}{l\vartheta_2}\left(\frac{\sqrt{-\Delta}}{2\vartheta_2} - \frac{\sqrt{-\Delta}\left(\theta_1 \cos\left(\frac{\sqrt{-\Delta}}{2}\eta\right) - \theta_2 \sin\left(\frac{\sqrt{-\Delta}}{2}\eta\right)\right)}{2\vartheta_2\left(\theta_1 \sin\left(\frac{\sqrt{-\Delta}}{2}\eta\right) + \theta_2 \cos\left(\frac{\sqrt{-\Delta}}{2}\eta\right)\right)}\right)^{-1} - \frac{3mk^2\Delta^2}{2l\vartheta_2^2}\left(\frac{\sqrt{-\Delta}}{2\vartheta_2} - \frac{\sqrt{-\Delta}\left(\theta_1 \cos\left(\frac{\sqrt{-\Delta}}{2}\eta\right) - \theta_2 \sin\left(\frac{\sqrt{-\Delta}}{2}\eta\right)\right)}{2\vartheta_2\left(\theta_1 \sin\left(\frac{\sqrt{-\Delta}}{2}\eta\right) + \theta_2 \cos\left(\frac{\sqrt{-\Delta}}{2}\eta\right)\right)}\right)^{-2} + \frac{2mk^2\Delta}{l}. \tag{87}$$

where $\eta = k\left(x + y - \frac{\nu\left(t + \frac{1}{\Gamma(\beta)}\right)^{\beta}}{\beta}\right)$, $\eta = k\left(x + y + \frac{\Gamma(\gamma+1)}{\beta}t^{\beta}\right)$ and $\eta = k\left(x + y + \frac{\nu}{\beta}t^{\beta}\right)$ are the three different wave transformations for all the 12 solution sets as specified earlier.

5 Graphical Illustration and Confab

This study uses various fractional derivative procedures to solve the NLWKB equation in (2 + 1)-dimension. The results are attained be employing the novel modified (G'/G^2)-expansion method, a consistent integration procedure applied to Beta, conformable, and M-truncated derivatives. This method generates several solutions for three different derivative operators, presented through 2D simple and time evolution plots, as well as 3D graphical representations. As a result, several types of optical solitary wave solutions, comprising bright-type, W-type, and dark-type solitons, are obtained. The use of 2D time evolution visualizations enables a clear comparison between the Beta-Derivative and the further two fractional derivatives, namely, the Conformable and M-Truncated Derivative. It is observed that varying the fractional derivative significantly affects wave motion without altering the overall shape of the curve, thereby illustrating the symmetry of their traveling wave solutions. A single solution may lead to the development of many distinct types of solutions if the parameter values take on various specific values. The novel modified (G'/G^2)-expansion method was used to generate soliton solutions. They provide a visual representation of the spatial and temporal dynamics of solitary waves. The graphs of the analytical solution (Figs. 1–3) make it evident that the novel modified (G'/G^2)-expansion method is a robust and efficient technique.

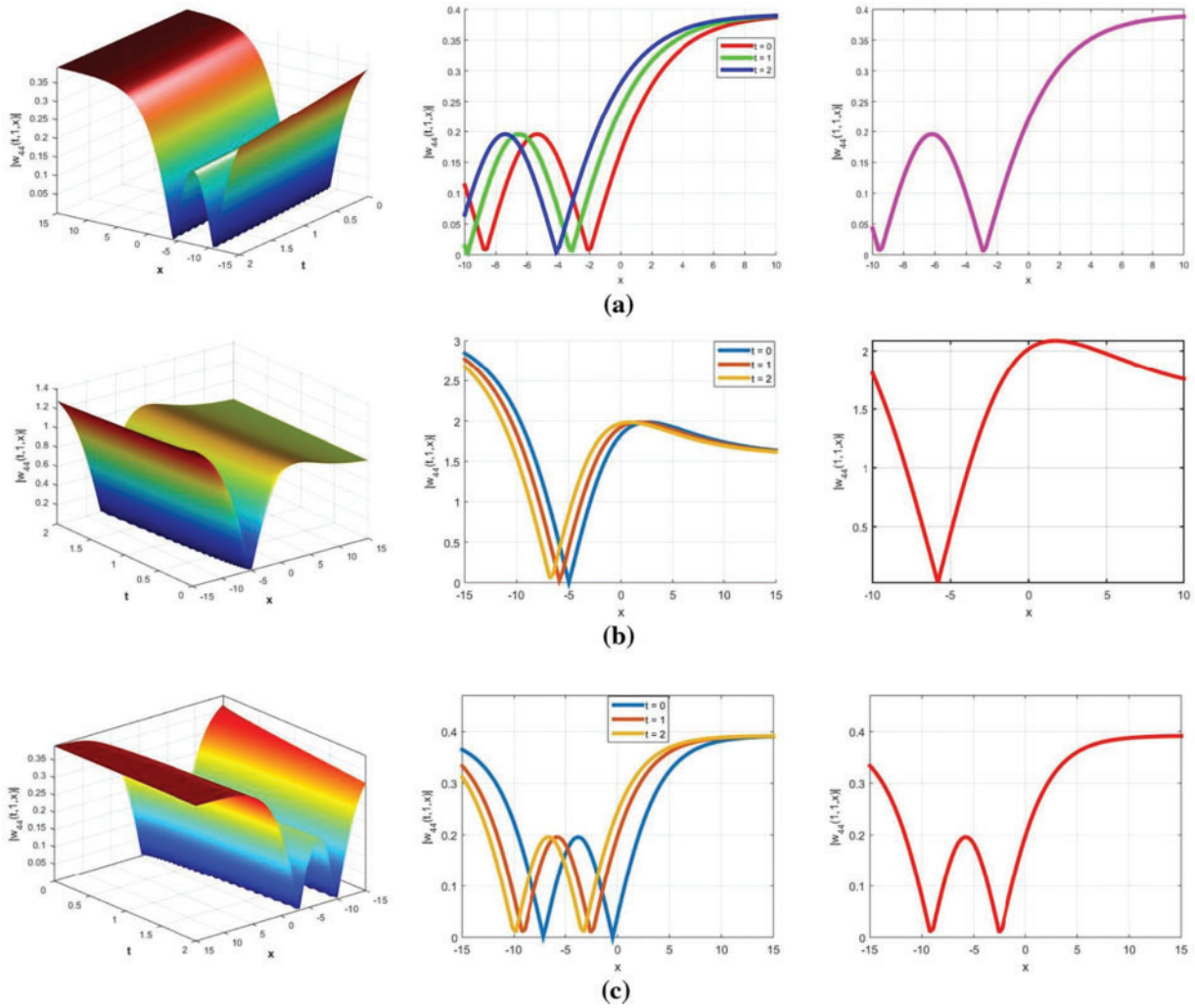

Figure 1: 2D with time evolution plots and 3D plots for soliton solution w_{44}. (a) β-derivative with $\beta = 0.5$, (b) M-Truncated derivative with $\beta = 0.5$, and $\gamma = 0.6$, (c) CD with $\beta = 0.5$

In Fig. 1a–c, for $\vartheta_1 = 0.2, \vartheta_2 = 0.1, \vartheta_3 = 2, \theta_1 = 1, \theta_2 = 2$, $l = 0.2$, $m = 0.5$, $n = 0.5$, $k = 0.2$, the bright soliton solutions demonstrate how different fractional-order derivatives affect the wave propagation. Beta derivatives produce the most compact solitons, while M-truncated derivatives introduce moderate dispersion, and conformable derivatives raise wave oscillations.

In Fig. 2a–c, for $\vartheta_1 = 0.2, \vartheta_2 = 0.1, \vartheta_3 = 2, \theta_1 = 1, \theta_2 = 2, l = 0.2, m = 0.5, n = 0.5, k = 0.2$, the W-type soliton solutions display that the Beta derivative holds strong localization, while the M-Truncated derivative smoothens, and the Conformable derivative disperses the soliton.

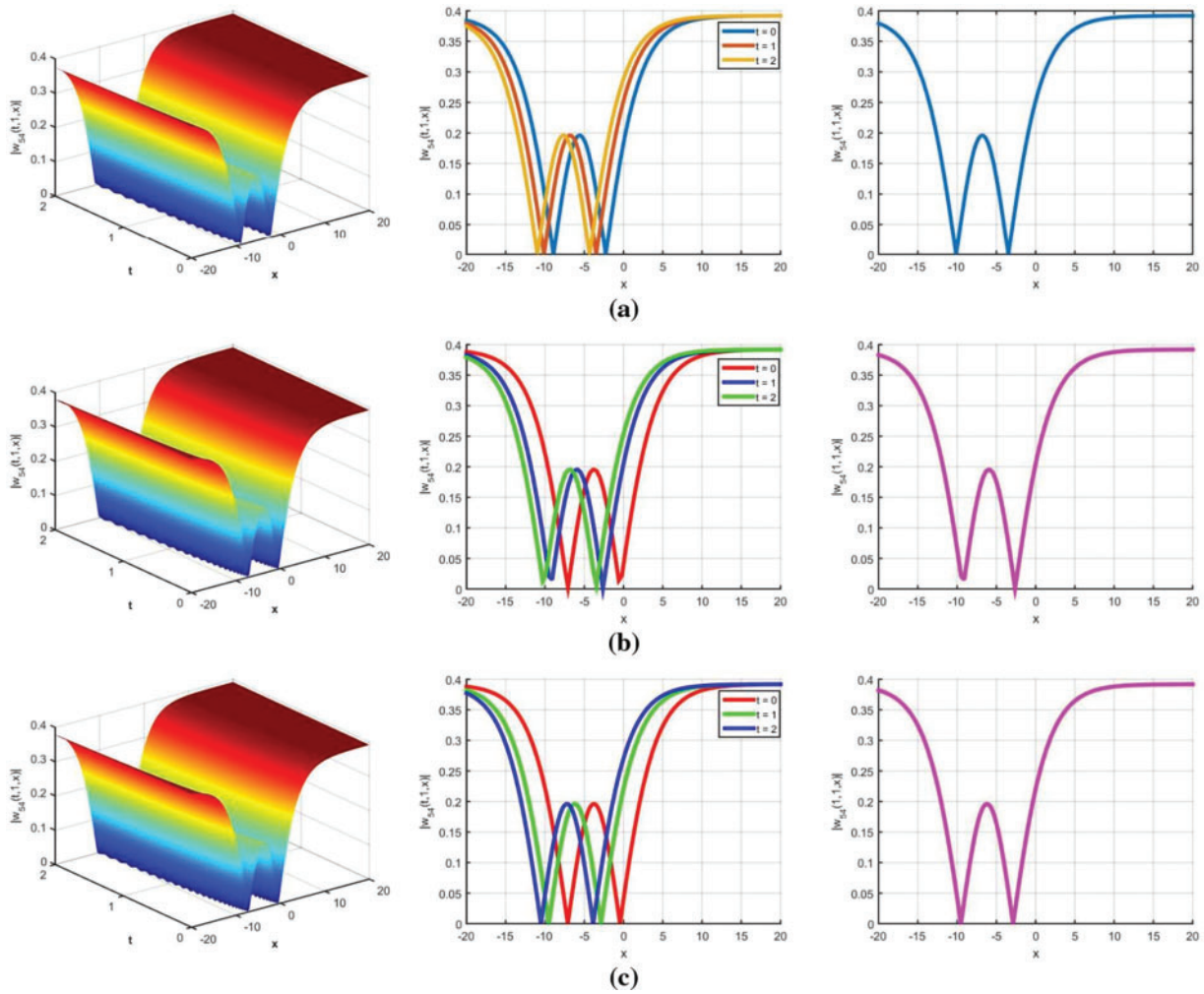

Figure 2: 2D with time evolution plots and 3D plots for soliton solution w_{54}. (a) β-derivative with $\beta = 0.5$, (b) M-Truncated derivative with $\beta = 0.5$, and $\gamma = 0.6$, (c) CD with $\beta = 0.5$

In Fig. 3a–c, for $\vartheta_1 = 0.2, \vartheta_2 = 0.1, \vartheta_3 = 2, \theta_1 = 1, \theta_2 = 2$, $l = 0.2$, $m = 0.5$, $n = 0.5$, $k = 0.2$, the dark soliton solutions show that the beta derivative maintains a compact, sharp soliton, while the M-truncated and conformable derivatives expand and smooth the soliton structure.

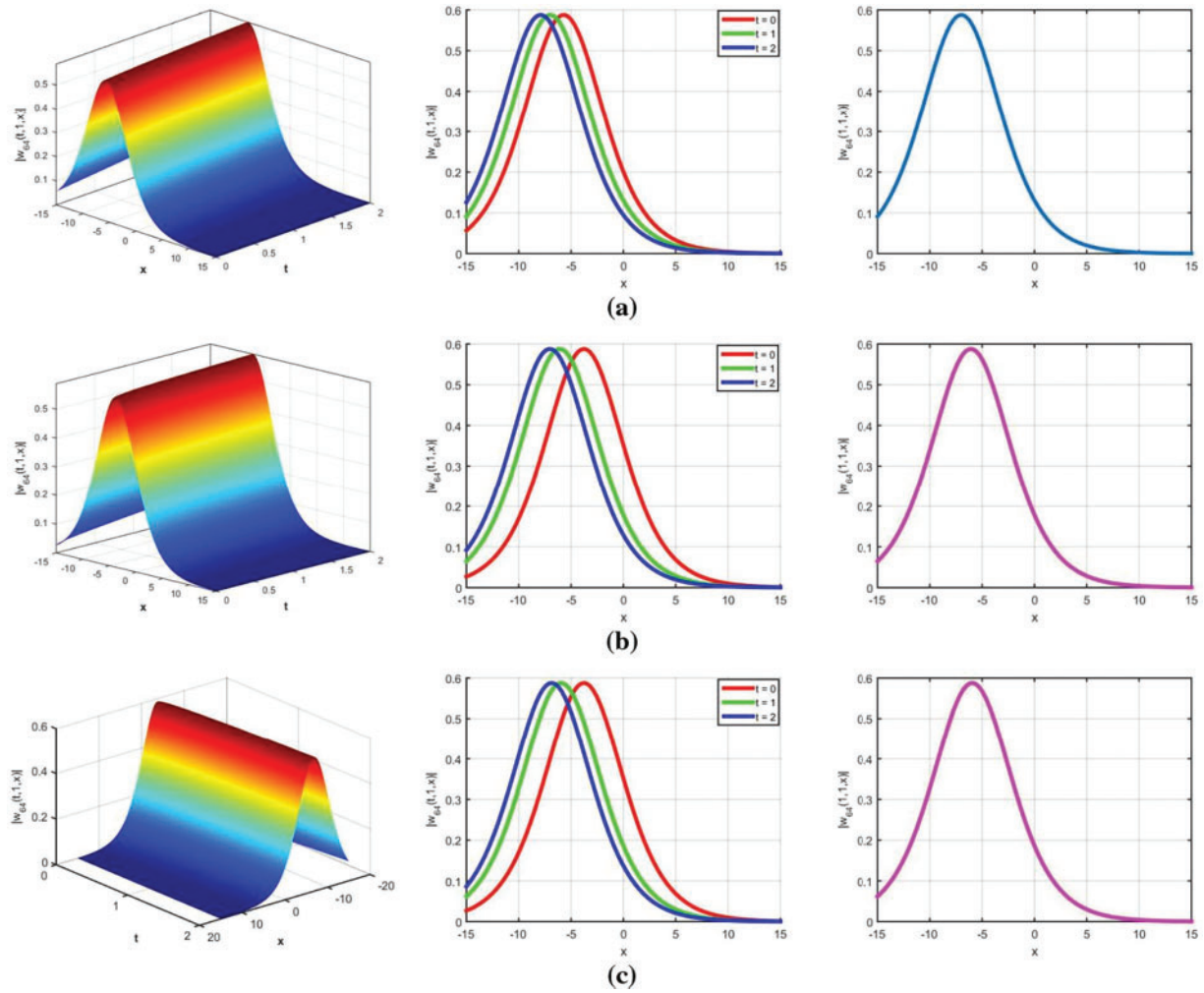

Figure 3: 2D with time evolution plots and 3D plots for soliton solution w_{64}. (a) β-derivative with $\beta = 0.5$, (b) M-Truncated derivative with $\beta = 0.5$, and $\gamma = 0.6$, (c) CD with $\beta = 0.5$

6 Bifurcation Analysis

Bifurcation analysis looks at the dynamics regardless of whether the parameters are inter-dependent and observes how the system behaves concerning different values. Using the Galilean transformation, the observed second differential Eq. (13) can be transformed into two first equations [48,49]:

$$\begin{cases} \dfrac{dw}{d\eta} = u \\ \dfrac{du}{d\eta} = \dfrac{1}{F_1}\left(-F_2 w^2 + F_3 w\right) \ , \end{cases} \tag{88}$$

where $F_1 = 4k^2 m$, $F_2 = 4l$, $F_3 = 4v^2 - 4v + n^2 - 4$.

The following set of equilibrium points makes up the system (88):

$$(0,0)\,,\ \left(\frac{F_3}{F_2},0\right).$$

Once we have the fixed points, we can analyze the stability of these points by computing the Jacobian matrix of the system (88). It is given by:

$$J\,(u,v)=\begin{vmatrix}0 & 1\\ \dfrac{-2F_2w+F_3}{F_1} & 0\end{vmatrix}=\frac{-2F_2w+F_3}{F_1}. \tag{89}$$

Jacobian gives a linear approximation of the system near the fixed or equilibrium points and helps classify these points as saddle points or center points based on the eigenvalues. This analysis is fundamental in understanding the local stability of a dynamical system.

The three phase portraits show the dynamics of the nonlinear system with different parameters and show the behavior of the trajectories in the phase space defined by w and u.

The phase portrait in Fig. 4 demonstrates a nonlinear system with two stable points (green dots) located at $(-1.17,\ 0)$ and $(1.07,\ 0)$, bounded by closed periodic trajectories and an unstable saddle point (red dot) located at $(0,\ 0)$ behaving as a separatrix. The closed loops about the stable points show bounded oscillatory motion, while the separatrix distributes the phase space into different basins of attraction. The center saddle point divides into two stable attractors, forming a double-well potential shape that looks like a figure-eight or a butterfly.

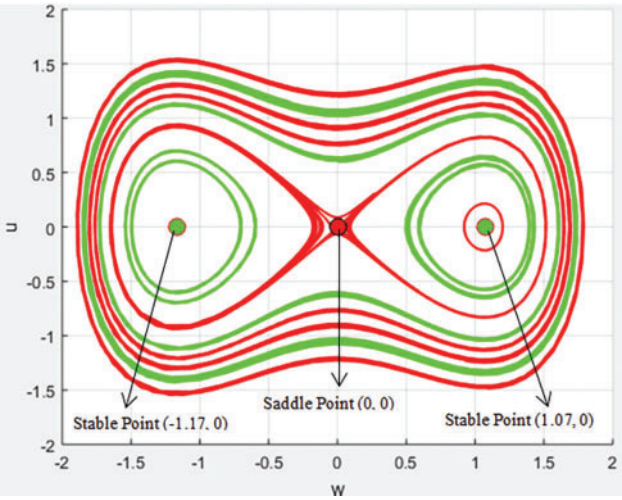

Figure 4: Phase Portrait of the system (88) when $k=1, m=1, l=1, v=0.2, n=0.1$

The phase portrait in Fig. 5 shows stable oscillatory behavior in the center at the origin $(0,\ 0)$. This center represents stability and shows that the nearby trajectory will return to equilibrium after a small perturbation. The closed and symmetrical contour around the center means a solid stability reflecting the restored properties of the system. The absence of saddle points further indicates the stability of the system, indicating the absence of unstable areas that could cause deviations. In general, the portrait shows good reliability, resulting in periodic behavior based on the parametric case.

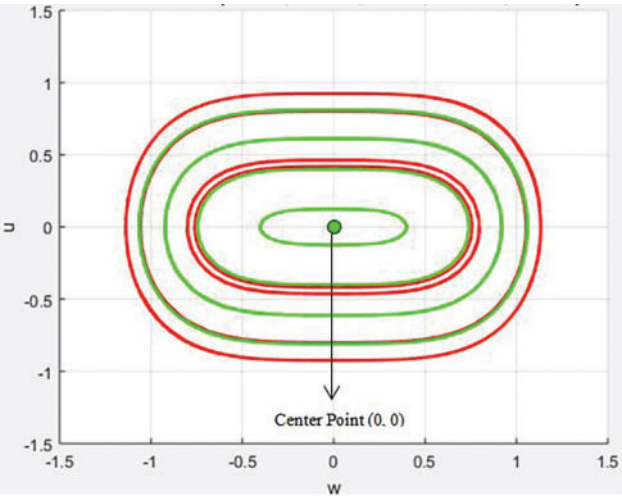

Figure 5: Phase Portrait of the system (88) when $k = 8, m = 1, l = 0.4, \nu = 0.2, n = 0.1$

The phase portrait in Fig. 6 illustrates two stable points (green dots) located at $(-2.45, 0)$ and $(1.35, 0)$ and an unstable saddle point (red dot) at the center $(0, 0)$, forming a figure-eight-shaped separatrix that divides the phase space into two basins of attraction. Trajectories near the stable points form closed loops, indicating periodic motion, while those near the separatrix are sensitive to initial conditions and may switch between basins. The system is globally stable within each basin but exhibits instability near the saddle point, highlighting the interplay of stability, energy levels, and nonlinear effects in determining the dynamics.

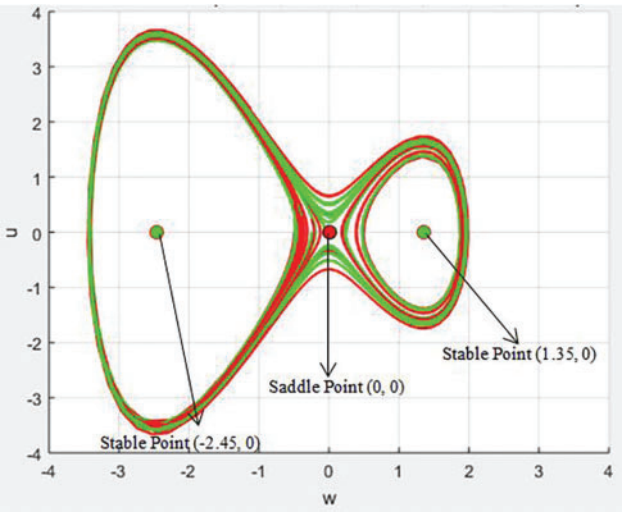

Figure 6: Phase Portrait of the system (88) when $k = 3, m = 0.5, l = 5, \nu = 5, n = 2$

7 Chaotic Analysis

In this section, we add an external force in the dynamical system (88) to make it perturbed as shown below:

$$\begin{cases} \dfrac{dw}{d\eta} = u \\ \dfrac{du}{d\eta} = \dfrac{1}{F_1}\left(-F_2 w^2 + F_3 w\right) + \rho \cos\left(\tau\, \eta\right), \end{cases} \tag{90}$$

where $\rho \cos(\tau\, \eta)$ is known as the perturbation term. In our system of equations, τ represents the frequency of the external perturbation, determining how often the external force oscillates over time, while ρ is the amplitude of the perturbation, controlling the strength of the external force [50]. The term $\rho\cos(\tau)$ models this periodic forcing. A higher τ means faster oscillations, and a larger ρ means a stronger force. Together, they define the nature of the perturbation, with stronger and more frequent forces potentially driving the system toward more complex or chaotic behavior, while weaker or slower perturbations tend to produce smoother, more regular dynamics.

The 2D and 3D chaotic phase portraits of the nonlinear dynamical system (90) in Fig. 7a,b show high sensitivity to initial conditions, which is the main characteristic of deterministic chaos. The butterfly-shaped 2D attractor and spiralling 3D trajectory recommend that the system oscillates between two stable regions but never settles, confirming non-periodic, bounded chaos for $\rho = 1.5$ and $\tau = 0.1$.

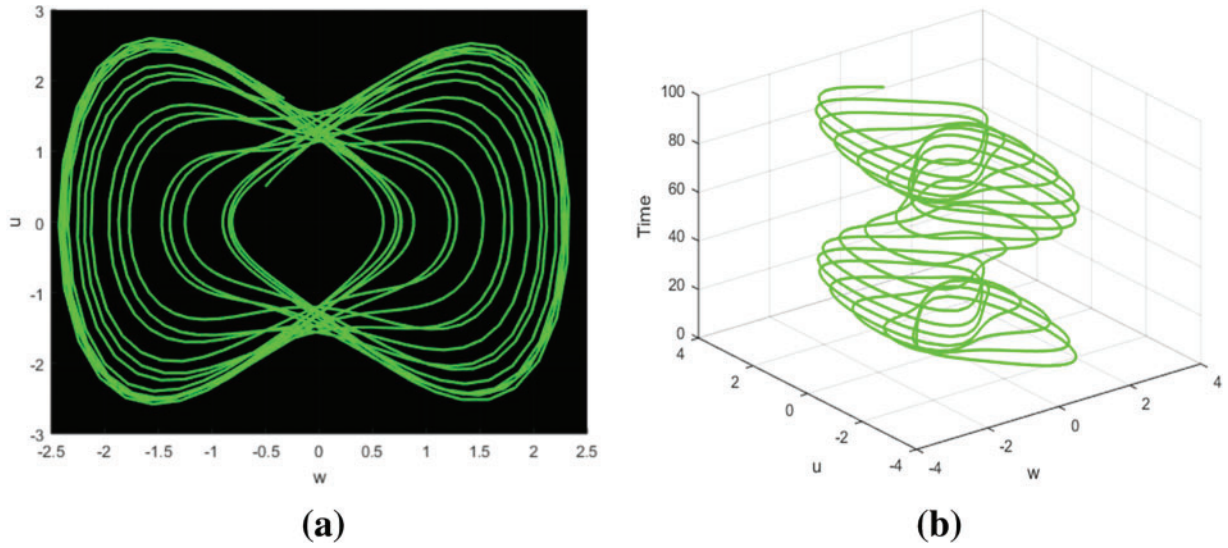

Figure 7: Chaotic analysis of the dynamic system (90) for $\rho = 1.5$ and $\tau = 0.1$. (a) 2D phase portrait; (b) 3D phase portrait

The 2D and 3D chaotic phase portraits of the nonlinear dynamical system (90) in Fig. 8a,b illustrate non-periodic, chaotic motion with bounded trajectories. The nested loops in 2D and increasing spirals in 3D affirm the presence of a quasi-periodic chaos for $\rho = 0.5$ and $\tau = 2.5$.

The 2D and 3D chaotic phase portraits of the nonlinear dynamical system (90) in Fig. 9a,b demonstrate bounded chaotic motion, where trajectories never repeat but remain bounded. The 2D elliptical trajectories and 3D spirals attractor affirm quasi-periodic chaos for $\rho = 0.5$ and $\tau = 1.5$.

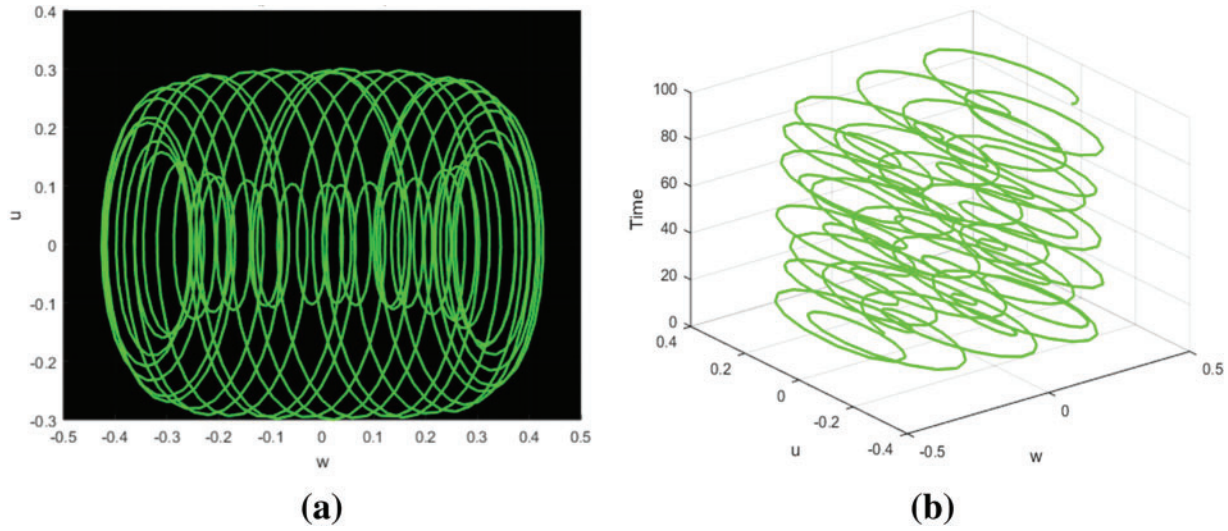

Figure 8: Chaotic analysis of the dynamic system (90) for $\rho = 0.5$ and $\tau = 2.5$. (a) 2D phase portrait; (b) 3D phase portrait

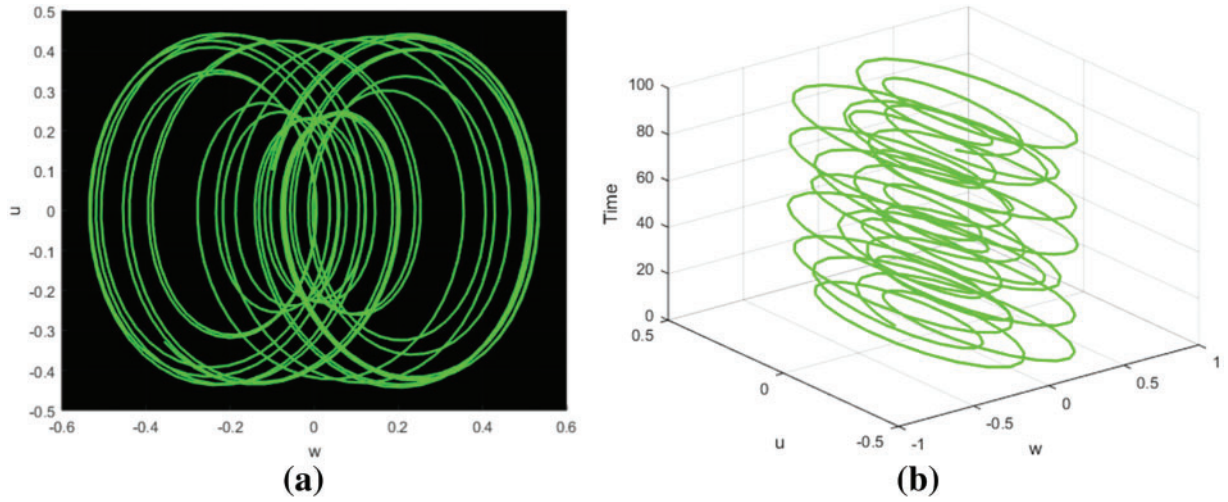

Figure 9: Chaotic analysis of the dynamic system (90) for $\rho = 0.5$ and $\tau = 1.5$. (a) 2D phase portrait; (b) 3D phase portrait

8 Time Series Analysis

Time analysis is performed to understand how a system evolves, identify patterns such as periodicity, chaos, or damping, and assess the stability of the system. It helps in predicting future behavior and determining the system's response to varying conditions [51].

The time series plots in Fig. 10a,b for $\rho = 1.5$ and $\tau = 0.1$ verify chaotic behavior, where both w and u display irregular, non-periodic oscillations over time. The system never forms a simple cycle, confirming the chaotic behavior detected in Fig. 7.

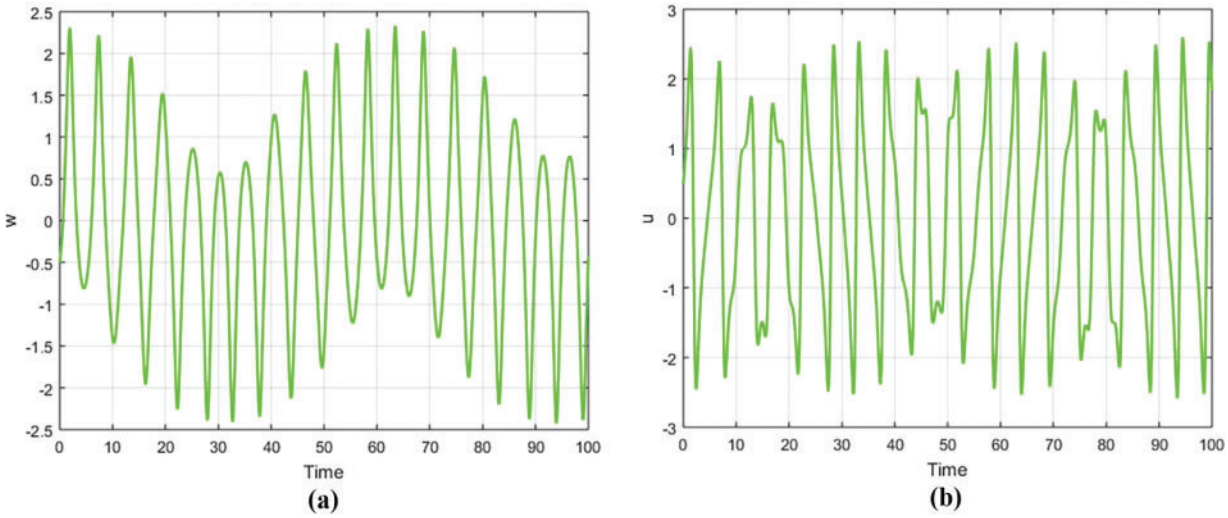

Figure 10: Time analysis for nonlinear dynamic system (90) for $\rho = 1.5$ and $\tau = 0.1$ (corresponding to Fig. 7). (a) Time series plot of w and time; (b) Time series plot of u and time

The time series plots in Fig. 11a,b for $\rho = 0.5$ and $\tau = 2.5$ verify chaotic, non-periodic behavior in the system. The w follows quasi-periodic oscillations, while the u displays highly irregular oscillations, demonstrating chaos. These remarks further support the chaotic behaviour observed in Fig. 8.

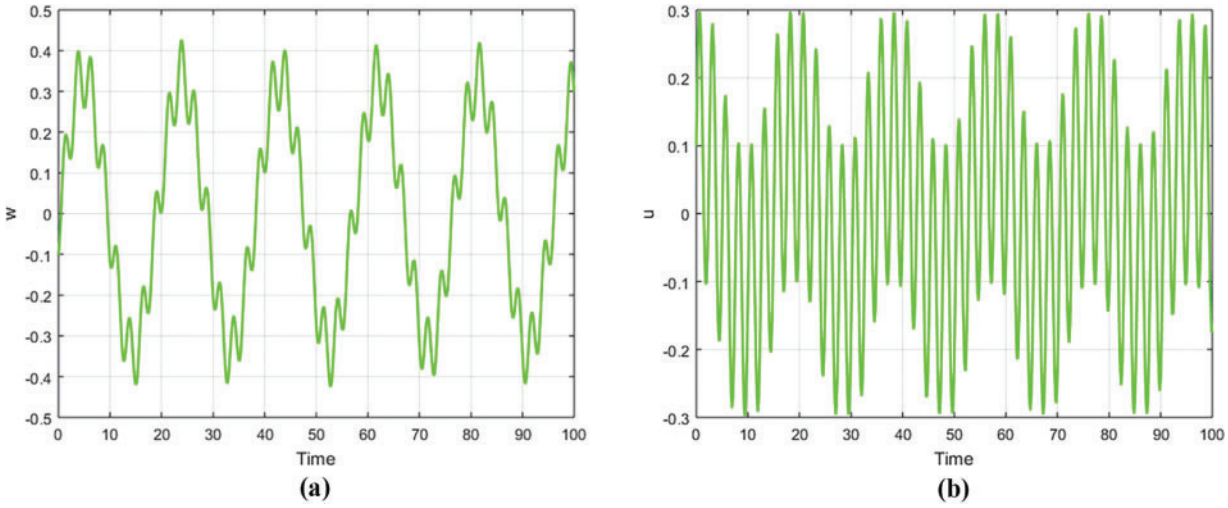

Figure 11: Time analysis for nonlinear dynamic system (90) for $\rho = 0.5$ and $\tau = 2.5$ (corresponding to Fig. 8). (a) Time series plot of w and time; (b) Time series plot of u and time

The time series plots in Fig. 12a,b for $\rho = 0.5$ and $\tau = 1.5$ verify chaotic or quasi-periodic motion, with bounded but irregular oscillations in both w and u. The non-repeating oscillations and sensitivity of the system on initial conditions show that the system follows a strange attractor, as observed in Fig. 9.

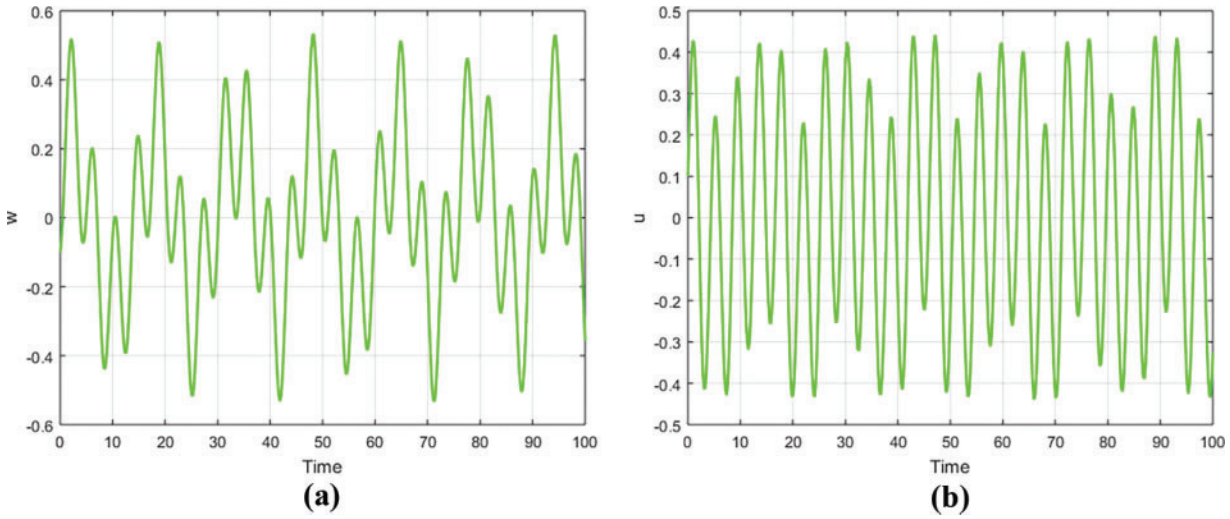

Figure 12: Time analysis for nonlinear dynamic system (90) for $\rho = 0.5$ and $\tau = 1.5$ (corresponding to Fig. 9). (a) Time series plot of w and time; (b) Time series plot of u and time

9 Multistability

Multistability refers to the presence of multiple stable states or behaviors that a dynamical system can exhibit under the same set of system parameters. It shows that the system can settle into different long-term behaviors depending on its initial conditions. In a multistable system, different trajectories can lead to periodic, quasi-periodic, or chaotic outcomes, even though the system's parameters remain unchanged. This phenomenon highlights how sensitive the system is to initial conditions, where small variations in starting points can result in vastly different dynamics [52].

In practical terms, multistability is important because it indicates that the system can respond to perturbations or initial differences in a variety of ways, revealing complex underlying structures like attractors. It is commonly observed in systems like biological processes, climate dynamics, and mechanical systems, where different operational modes can coexist.

The multistability plots in Fig. 13a,b for $\rho = 0.5$, $\tau = 2.5$ show three distinct basins of attraction, with trajectories (red, green, blue) corresponding to three different initial conditions for $\rho = 0.5$, $\tau = 2.5$. The red trajectories form the outermost attractor with large amplitude oscillations, while the green and blue trajectories are nested within, indicating smaller, localized oscillations. The system remains stable and bounded, with no overlap between attractors, reflecting well-defined basins of attraction. This demonstrates the system's multistable nature, where initial conditions determine which attractor the system converges to, driven by nonlinear dynamics and external forcing.

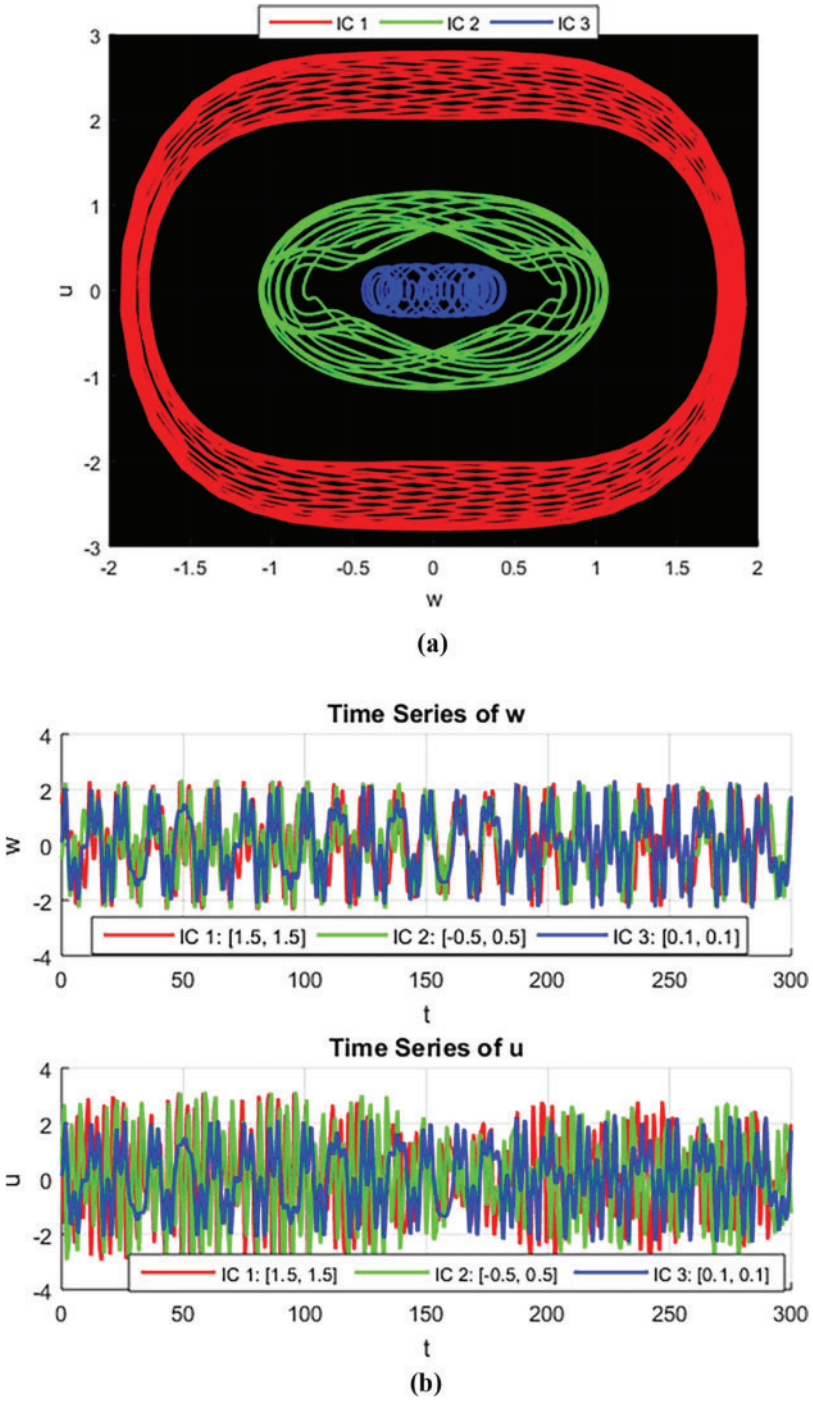

Figure 13: (a) Multistability analysis for the perturbed system (90) for $\rho = 0.5$, $\tau = 2.5$ at different initial conditions [1.5, 1.5], [−0.5, 0.5], [0.1, 0.1]; (b) Time series analysis of w vs. t and u vs. t

10 Poincaré Analysis

Poincaré Analysis (often associated with Poincaré sections or Poincaré maps) is a powerful technique used in the study of dynamical systems, especially for analyzing systems exhibiting periodic, quasi-periodic, or chaotic behavior. It is named after the French mathematician Henri Poincaré, who made significant contributions to the study of celestial mechanics and dynamical systems. It helps in identifying periodicity, stability, or chaotic behavior in systems [53].

The 2D and 3D Poincaré maps in Fig. 14a,b for $\rho = 0.5$, $\tau = 2\pi$ verify quasi-periodic behavior, where the system's behavior remains structured yet non-repeating over time. The absence of chaotic scattering shows that the system forms a clear, convergent trajectory, making it deterministic but non-periodic.

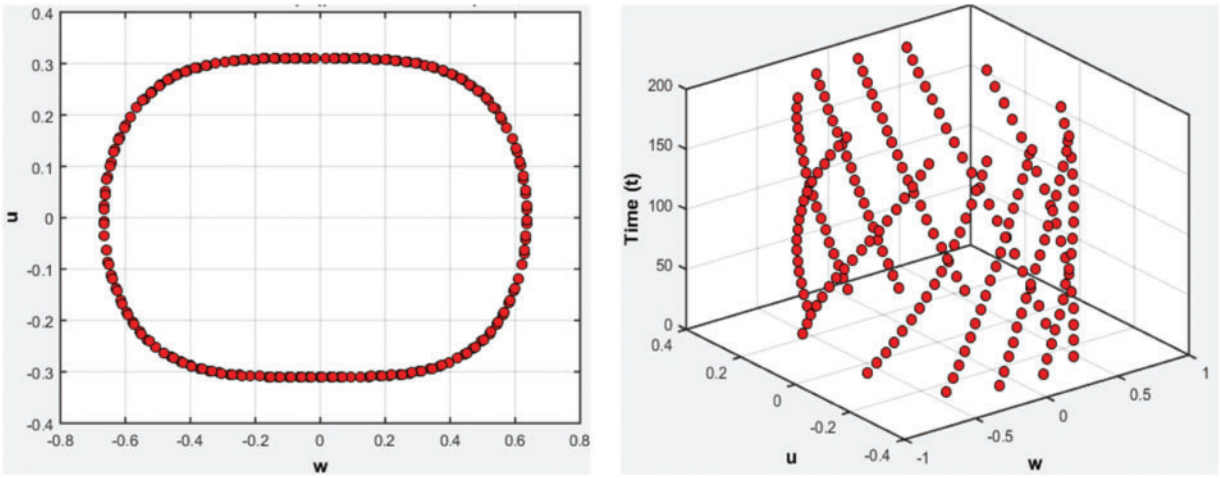

(a) (b)

Figure 14: (a) 2D Poincaré Map of the perturbed system (90) for $\rho = 0.5$, $\tau = 2\pi$, with initial condition [0.3, 0.3]; (b) 3D Poincaré Map of the perturbed system (90)

The 2D Poincaré map in Fig. 15a shows a closed, teardrop-shaped structure, showing a quasi-periodic behavior with a well-defined pattern for $\rho = 1.5$, $\tau = 4\pi$. In Fig. 15b, the 3D Poincaré map illustrates a layered and spiraling structure, showing a deterministic but non-repeating motion. These maps confirm the quasi-periodic behavior of the system, where trajectories remain bounded but never settle into a fixed periodic orbit.

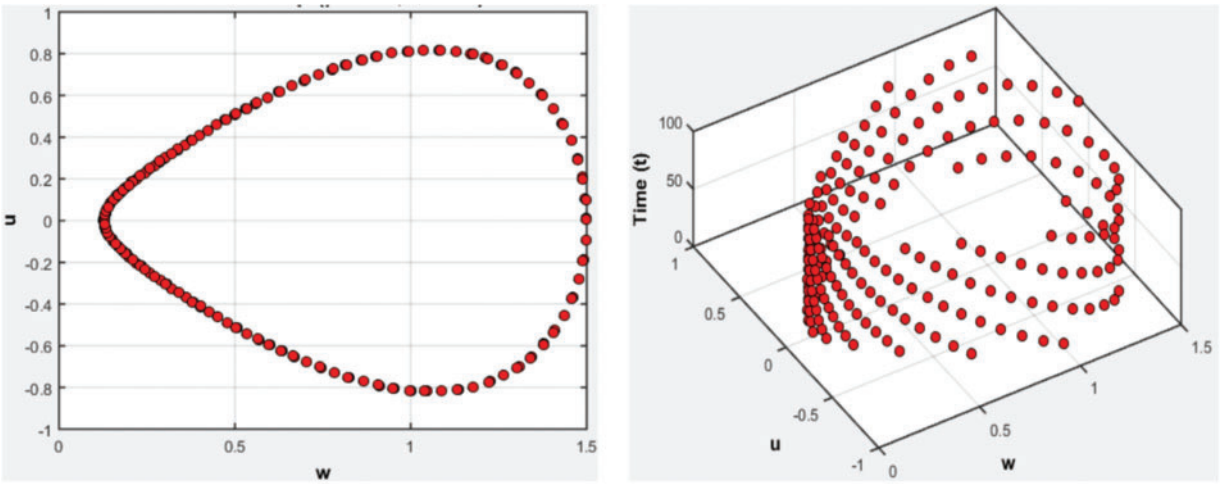

(a) (b)

Figure 15: (a) 2D Poincaré Map of the perturbed system (90) for $\rho = 1.5$, $\tau = 4\pi$, with initial condition [0.3, 0.3]; (b) 3D Poincaré Map of the perturbed system (90)

11 Conclusion

The novel modified (G'/G^2)-expansion method has been successfully used to derive new traveling wave solutions for the (2 + 1)-dimensional nonlinear Wazwaz Kaur Boussinesq equation. By using fractional derivatives, i.e., Conformable, Beta, and M-truncated derivatives, we have generated various soliton solutions, including W-type, bright-type, and dark-type solitons, which demonstrate the flexibility of this approach in solving nonlinear fractional differential equations. Bifurcation analysis reveals the system's sensitivity to parameter changes, showing how small adjustments can trigger transitions from stable periodic behavior to chaotic dynamics. Chaotic analysis further confirms this, demonstrating how external forcing induces complex, unpredictable behaviors, such as sensitive dependence on initial conditions and the formation of strange attractors. Multistability analysis highlights the system's ability to settle into multiple stable states, emphasizing the critical role of initial conditions in determining long-term dynamics. Finally, Poincaré's analysis uncovers how external forcing influences the system, revealing periodic behavior at lower forcing amplitudes and more complex dynamics at higher forces. The findings of this study have significant implications for practical applications in fields such as tidal wave propagation, tsunami modeling, optical communication, and nonlinear wave phenomena. The dynamic analysis of bifurcation, chaos, multistability, and Poincaré maps not only enhances our understanding of soliton dynamics but also provides a comprehensive framework for predicting and controlling the behavior of complex systems. Unlike previous studies, this study advances the field by using the novel modified (G'/G^2)-expansion method, providing a more generalized framework for developing soliton solutions in fractional systems. These findings enhance the comprehension of nonlinear wave propagation, offering significant insights for practical applications such as optical fibers, plasma physics, and fluid dynamics. Moreover, the study differentiates chaotic analysis, which unveils irregular and aperiodic behavior, from multistability, where multistable states co-occur under the same parameters. This distinction highlights the complex, dynamic nature of the system. Furthermore, this study paves the way for future research, including applications

to higher-dimensional nonlinear models, advanced fractional wave equations, and coupled soliton systems, contributing to progress in nonlinear science and engineering.

This study confesses certain limitations, such as the need for further investigation of higher dimension nonlinear models and more complex fractional equations. Future research can focus on expanding the methodology to coupled systems and investigating nonlinear phenomena under various parameter limitations, improving the applicability of results in a wider range of scientific and technical fields.

Acknowledgement: The authors would like to thank the Editor and Reviewers for their valuable comments, which have helped improve the quality of the paper.

Funding Statement: The authors received no specific funding for this study.

Author Contributions: Study conception and design: Amna Mumtaz and Abdul Manan; data collection: Muhammad Shakeel; analysis and interpretation of results: Amna Mumtaz, Muhammad Shakeel and Nehad Ali Shah; draft manuscript preparation: Amna Mumtaz, Muhammad Shakeel, Abdul Manan and Nehad Ali Shah. All authors reviewed the results and approved the final version of the manuscript.

Availability of Data and Materials: The data that supports the findings of this study are available from the corresponding author upon reasonable request.

Ethics Approval: Not applicable.

Conflicts of Interest: The authors declare no conflicts of interest to report regarding the present study.

References

1. Arshed S, Rahman RU, Raza N, Khan AK, Inc M. A variety of fractional soliton solutions for three important coupled models arising in mathematical physics. Int J Mod Phys B. 2022;36(1):2250002. doi:10.1142/s0217979222500023.
2. Arefin MA, Sadiya U, Inc M, Uddin MH. Adequate soliton solutions to the space-time fractional telegraph equation and modified third-order KdV equation through a reliable technique. Opt Quantum Electron. 2022;54(5):309. doi:10.1007/s11082-022-03640-9.
3. Sadiya U, Inc M, Arefin MA, Uddin MH. Consistent travelling waves solutions to the non-linear time fractional Klein-*Gordon* and Sine-*Gordon* equations through extended tanh-function approach. J Taibah Univ Sci. 2022;16(1):594–607. doi:10.1080/16583655.2022.2089396.
4. Zaman UM, Arefin MA, Akbar MA, Uddin MH. Study of the soliton propagation of the fractional nonlinear type evolution equation through a novel technique. PLoS One. 2023;18(5):e0285178. doi:10.1371/journal.pone.0285178.
5. Zaman UHM, Arefin MA, Ali Akbar M, Uddin MH. Analyzing numerous travelling wave behavior to the fractional-order nonlinear Phi-4 and Allen-Cahn equations throughout a novel technique. Results Phys. 2022;37:105486. doi:10.1016/j.rinp.2022.105486.
6. Aljahdaly NH, Shah R, Naeem M, Arefin MA. A comparative analysis of fractional space-time advection-dispersion equation via semi-analytical methods. J Funct Spaces. 2022;2022:4856002. doi:10.1155/2022/4856002.

7. Khatun MA, Arefin MA, Ali Akbar M, Uddin MH. Numerous explicit soliton solutions to the fractional simplified Camassa-Holm equation through two reliable techniques. Ain Shams Eng J. 2023;14(12):102214. doi:10.1016/j.asej.2023.102214.
8. Arefin MA, Khatun MA, Islam MS, Ali Akbar M, Uddin MH. Explicit soliton solutions to the fractional order nonlinear models through the atangana beta derivative. Int J Theor Phys. 2023;62(6):134. doi:10.1007/s10773-023-05400-1.
9. Khatun MA, Arefin MA, Uddin MH, Inc M, Akbar MA. An analytical approach to the solution of fractional-coupled modified equal width and fractional-coupled Burgers equations. J Ocean Eng Sci. 2022;175:704. doi:10.1016/j.joes.2022.03.016.
10. Qureshi S, Chang MM, Shaikh AA. Analysis of series RL and RC circuits with time-invariant source using truncated M, Atangana beta and conformable derivatives. J Ocean Eng Sci. 2021;6(3):217–27. doi:10.1016/j.joes.2020.11.006.
11. Almeida R. A Caputo fractional derivative of a function with respect to another function. Commun Nonlinear Sci Numer Simul. 2017;44:460–81. doi:10.1016/j.cnsns.2016.09.006.
12. da C Sousa JV, de Oliveira E C. On the ψ-hilfer fractional derivative. Commun Nonlinear Sci Numer Simul. 2018;60:72–91. doi:10.1016/j.cnsns.2018.01.005.
13. Romero LG, Luque LL, Dorrego GA, Cerutti RA. On the k-Riemann-Liouville fractional derivative. Int J Contemp Math Sci. 2013;8:41–51. doi:10.12988/ijcms.2013.13004.
14. Jumarie G. Modified Riemann-Liouville derivative and fractional Taylor series of nondifferentiable functions further results. Comput Math Appl. 2006;51(9–10):1367–76. doi:10.1016/j.camwa.2006.02.001.
15. Ali A, Seadawy AR. Dispersive soliton solutions for shallow water wave system and modified Benjamin-Bona-Mahony equations via applications of mathematical methods. J Ocean Eng Sci. 2021;6(1):85–98. doi:10.1016/j.joes.2020.06.001.
16. Malfliet W. The tanh method: a tool for solving certain classes of nonlinear evolution and wave equations. J Comput Appl Math. 2004;164:529–41. doi:10.1016/S0377-0427(03)00645-9.
17. Ablowitz MJ, Clarkson PA. Solitons, nonlinear evolution equations and inverse scattering transform. London, UK: Cambridge University Press; 1991.
18. He JH, Wu XH. Exp-function method for nonlinear wave equations. Chaos Sol Fractals. 2006;30(3):700–8. doi:10.1016/j.chaos.2006.03.020.
19. Shakeel M, Iqbal MA, Din Q, Hassan QM, Ayub K. New exact solutions for coupled nonlinear system of ion sound and Langmuir waves. Indian J Phys. 2020;94(6):885–94. doi:10.1007/s12648-019-01522-7.
20. Shakeel M, Attaullah, Shah NA, Chung JD. Modified exp-function method to find exact solutions of microtubules nonlinear dynamics models. Symmetry. 2023;15(2):360. doi:10.3390/sym15020360.
21. Shakeel M, Attaullah, Shah NA, Chung JD. Application of modified exp-function method for strain wave equation for finding analytical solutions. Ain Shams Eng J. 2023;14(3):101883. doi:10.1016/j.asej.2022.101883.
22. Shakeel M, Mohyud-Din ST, Iqbal MA. Closed form solutions for coupled nonlinear Maccari system. Comput Math Appl. 2018;76(4):799–809. doi:10.1016/j.camwa.2018.05.020.
23. Ahmad J, Rezazadeh H. New analytical wave structures for some nonlinear dynamical models via mathematical technique. Univ Wah J Sci Technol. 2023;7(1):51–75.
24. Ma WX, Huang T, Zhang Y. A multiple exp-function method for nonlinear differential equations and its application. Phys Scr. 2010;82(6):065003. doi:10.1088/0031-8949/82/06/065003.
25. Arshed S, Sadia M. (G'/G^2)-expansion method: new traveling wave solutions for some nonlinear fractional partial differential equations. Opt Quantum Electron. 2018;50(3):123. doi:10.1007/s11082-018-1391-6.
26. Nisar KS, Inc M, Jhangeer A, Muddassar M, Infal B. New soliton solutions of Heisenberg ferromagnetic spin chain model. Pramana. 2022;96(1):28. doi:10.1007/s12043-021-02266-y.

27. Mumtaz A, Shakeel M, Alshehri M, Ali Shah N. New analytical technique for prototype closed form solutions of certain nonlinear partial differential equations. Results Phys. 2024;60:107640. doi:10.1016/j.rinp.2024.107640.
28. Ali A, Ahmad J, Javed S. Exploring the dynamic nature of soliton solutions to the fractional coupled nonlinear Schrodinger model with their sensitivity analysis. Opt Quantum Electron. 2023;55(9):810. doi:10.1007/s11082-023-05033-y.
29. Akram S, Ahmad J, Rehman SU, Younas T. Stability analysis and dispersive optical solitons of fractional Schrödinger-Hirota equation. Opt Quantum Electron. 2023;55(8):664. doi:10.1007/s11082-023-04942-2.
30. Seadawy AR, Alsaedi BA. Dynamical stricture of optical soliton solutions and variational principle of nonlinear Schrödinger equation with Kerr law nonlinearity. Mod Phys Lett B. 2024;38(28):2450254. doi:10.1142/S0217984924502543.
31. Seadawy AR, Alsaedi BA. Variational principle and optical soliton solutions for some types of nonlinear Schrödinger dynamical systems. Int J Geom Methods Mod Phys. 2024;21(6):2430004. doi:10.1142/S0219887824300046.
32. Younas U, Hussain E, Muhammad J, Sharaf M, Meligy ME. Chaotic structure, sensitivity analysis and dynamics of solitons to the nonlinear fractional longitudinal wave equation. Int J Theor Phys. 2025;64(2):42. doi:10.1007/s10773-025-05916-8.
33. Ismael HF, Sulaiman TA, Nabi HR, Younas U. On the study of dynamical wave's nature to generalized (3 + 1)-dimensional variable-coefficient Kadomtsev-Petviashvili equation: application in the plasma and fluids. Nonlinear Dyn. 2025;113(3):2653–65. doi:10.1007/s11071-024-10338-y.
34. Jhangeer A, Almusawa H, Hussain Z. Bifurcation study and pattern formation analysis of a nonlinear dynamical system for chaotic behavior in traveling wave solution. Results Phys. 2022;37:105492. doi:10.1016/j.rinp.2022.105492.
35. Ak T, Saha A, Dhawan S. Performance of a hybrid computational scheme on traveling waves and its dynamic transition for Gilson-Pickering equation. Int J Mod Phys C. 2019;30(4):1950028. doi:10.1142/S0129183119500281.
36. Ali MN, Husnine SM, Saha A, Bhowmik SK, Dhawan S, Ak T. Exact solutions, conservation laws, bifurcation of nonlinear and supernonlinear traveling waves for Sharma–Tasso–Olver equation. Nonlinear Dyn. 2018;94(3):1791–801. doi:10.1007/s11071-018-4457-x.
37. Dubinov AE, Kolotkov DY, Sazonkin MA. Supernonlinear waves in plasma. Plasma Phys Rep. 2012;38(10):833–44. doi:10.1134/S1063780X12090036.
38. Almusawa H, Jhangeer A, Hussain Z. Observation on different dynamics of breaking soliton equation by bifurcation analysis and multistability theory. Results Phys. 2022;36:105364. doi:10.1016/j.rinp.2022.105364.
39. Rehman ZU, Hussain Z, Li Z, Abbas T, Tlili I. Bifurcation analysis and multi-stability of chirped form optical solitons with phase portrait. Results Eng. 2024;21:101861. doi:10.1016/j.rineng.2024.101861.
40. Parker TS, Chua L. Practical numerical algorithms for chaotic systems. Berlin/Heidelberg, Germany: Springer; 2012.
41. Ansar R, Abbas M, Mohammed PO, Al-Sarairah E, Gepreel KA, Soliman MS. Dynamical study of coupled Riemann wave equation involving conformable, beta, and M-truncated derivatives via two efficient analytical methods. Symmetry. 2023;15(7):1293. doi:10.3390/sym15071293.
42. Khalil R, Al Horani M, Yousef A, Sababheh M. A new definition of fractional derivative. J Comput Appl Math. 2014;264:65–70. doi:10.1016/j.cam.2014.01.002.
43. Hussain A, Jhangeer A, Abbas N, Khan I, Sherif EM. Optical solitons of fractional complex Ginzburg-Landau equation with conformable, beta, and M-truncated derivatives: a comparative study. Adv Differ Eq. 2020;2020:612. doi:10.1186/s13662-020-03052-7.

44. Saboor A, Shakeel M, Liu X, Zafar A, Ashraf M. A comparative study of two fractional nonlinear optical model via modified (G'/G^2)-expansion method. Opt Quantum Electron. 2023;56(2):259. doi:10.1007/s11082-023-05824-3.
45. Vanterler CJ, Oliveira EC. A new truncated M-fractional derivative type unifying some fractional derivative types with classical properties. Int J Anal Appl. 2018;16(1):83–96. doi:10.28924/2291-8639-16-2018-83.
46. Shahen NHM, Foyjonnesa, Bashar MH, Ali MS, Mamun A-A. Dynamical analysis of long-wave phenomena for the nonlinear conformable space-time fractional (2 + 1)-dimensional AKNS equation in water wave mechanics. Heliyon. 2020;6(10):e05276. doi:10.1016/j.heliyon.2020.e05276.
47. Silambarasan R, Nisar KS. Doubly periodic solutions and non-topological solitons of (2 + 1)-dimension Wazwaz Kaur Boussinesq equation employing Jacobi elliptic function method. Chaos Sol Fract. 2023;175:113997. doi:10.1016/j.chaos.2023.113997.
48. Chow SN, Hale JK. Methods of bifurcation theory. Berlin/Heidelberg, Germany: Springer; 2012.
49. Riaz MB, Jhangeer A, Duraihem FZ, Martinovic J. Analyzing dynamics: lie symmetry approach to bifurcation, chaos, multistability, and solitons in extended (3 + 1)-dimensional wave equation. Symmetry. 2024;16(5):608. doi:10.3390/sym16050608.
50. Ganie AH, AlBaidani MM, Wazwaz AM, Ma WX, Shamima U, Ullah MS. Soliton dynamics and chaotic analysis of the Biswas-Arshed model. Opt Quantum Electron. 2024;56(8):1379. doi:10.1007/s11082-024-07291-w.
51. Jhangeer A, Beenish. Study of magnetic fields using dynamical patterns and sensitivity analysis. Chaos Sol Fract. 2024;182:114827. doi:10.1016/j.chaos.2024.114827.
52. Jhangeer A, Ali Faridi W, Alshehri M. The study of phase portraits, multistability visualization, Lyapunov exponents and chaos identification of coupled nonlinear volatility and option pricing model. Eur Phys J Plus. 2024;139(7):658. doi:10.1140/epjp/s13360-024-05435-1.
53. Jhangeer A, Beenish, Talafha AM, Ansari AR, Imran M. Analytical and dynamical analysis of nonlinear Riemann wave equation in plasma systems. Arab J Basic Appl Sci. 2024;31(1):536–53. doi:10.1080/25765299.2024.2408971.